

UNCLASSIFIED

AD NUMBER
AD920489
NEW LIMITATION CHANGE
TO Approved for public release, distribution unlimited
FROM Distribution authorized to U.S. Gov't. agencies only; Test and Evaluation; FEB 1974. Other requests shall be referred to Air Force Armament Lab, Attn: DLMA, Eglin AFB, FL 32542.
AUTHORITY
Air Force Armament Lab ltr dtd 1 Apr 1976

THIS PAGE IS UNCLASSIFIED

THIS REPORT HAS BEEN DELIMITED
AND CLEARED FOR PUBLIC RELEASE
UNDER DOD DIRECTIVE 5200.20 AND
NO RESTRICTIONS ARE IMPOSED UPON
ITS USE AND DISCLOSURE.

DISTRIBUTION STATEMENT A

APPROVED FOR PUBLIC RELEASE;
DISTRIBUTION UNLIMITED.

AFATL-TR-74-51

AD920489

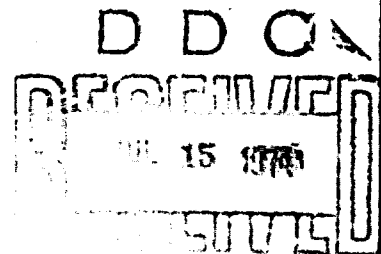
**METHODS FOR CALCULATING MAGNUS
FORCES ON SLENDER BODIES OF REVOLUTION**

UNIVERSITY OF FLORIDA

TECHNICAL REPORT AFATL-TR-74-51

FEBRUARY 1974

Distribution limited to U. S. Government agencies only; this report documents test and evaluation; distribution limitation applied February 1974. Other requests for this document must be referred to the Air Force Armament Laboratory (DLMA), Eglin Air Force Base, Florida 32542.



AIR FORCE ARMAMENT LABORATORY

AIR FORCE SYSTEMS COMMAND • UNITED STATES AIR FORCE

EGLIN AIR FORCE BASE, FLORIDA

Methods For Calculating Magnus Forces On Slender Bodies Of Revolution

J. E. Milton

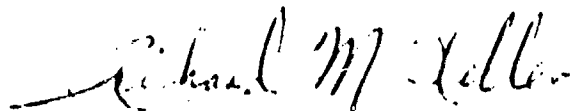
Distribution limited to U. S. Government agencies only;
this report documents test and evaluation; distribution
limitation applied February 1974. Other requests for
this document must be referred to the Air Force Armament
Laboratory (DLMA), Eglin Air Force Base, Florida 32542.

FOREWORD

This report was prepared by the Eglin Graduate Center, College of Engineering, University of Florida, Eglin Air Force Base, Florida, and covers work performed under Contract No. ✓ F08635-70-C-0065 with the Air Force Armament Laboratory, Eglin Air Force Base, Florida. The project monitor for the Armament Laboratory was Dr. George B. Findley (DLMA). The work described in this report commenced in February 1972 and was completed in December 1973.

The principal contributor was Dr. J. E. Milton.

This technical report has been reviewed and is approved.



RICHARD M. KELLER, Colonel, USAF
Chief, Air-to-Surface Modular
Guided Weapons Division

ABSTRACT

Theories for predicting the Magnus force for slender, pointed bodies of revolution at small angle of attack and small spin rates are reviewed. A semi-empirical method for calculating $C_{y,p}$ is discussed and shown to be applicable to a variety of bodies and experimental situations.

Distribution limited to U. S. Government agencies only; this report documents test and evaluation; distribution limitation applied February 1974. Other requests for this document must be referred to the Air Force Armament Laboratory (DLMA), Eglin Air Force Base, Florida 32542.

TABLE OF CONTENTS

Section		Page
I	INTRODUCTION	1
II	HISTORICAL DISCUSSION	2
III	PROPOSED THEORIES	5
IV	RESULTS	14
V	DISCUSSION AND CONCLUSIONS	36
	REFERENCES	38

LIST OF FIGURES

Figure	Title	Page
1	Coordinate System	6
2	Effective Shape	9
3	$C_{y,p}$ Versus α , Experimental and Calculated $M = 4.03$, $L/d = 24.88$, $R = \frac{960,000}{Cal}$	15
4	$C_{y,p}$ Versus α , Experimental and Calculated $M = 2.99$, $L/d = 24.88$, $R = \frac{619,000}{Cal}$	16
5	$C_{y,p}$ Versus α , Experimental and Calculated $M = 2.48$, $L/d = 7$, $R = 4 \times 10^6$	17
6	$C_{y,p}$ Versus α , Experimental and Calculated $M = 2.48$, $L/d = 5$, $R = 4 \times 10^6$	18
7	$C_{y,p}$ Versus α , Experimental and Calculated $M = 2.21$, $L/d = 7$, $R = \frac{333,000}{Cal}$	19
8	$C_{y,p}$ Versus α , Experimental and Calculated $M = 2.00$, $L/d = 10$, $R = \frac{316,000}{Cal}$	20
9	$C_{y,p}$ Versus α , Experimental and Calculated $M = 2.00$, $L/d = 8$, $R = \frac{316,000}{Cal}$	21
10	$C_{y,p}$ Versus α , Experimental and Calculated $M = 1.90$, $L/d = 7$, $R = \frac{426,000}{Cal}$	22
11	$C_{y,p}$ Versus α , Experimental and Calculated $M = 1.77$, $L/d = 7$, $R = 3.29 \times 10^6$	23
12	$C_{y,p}$ Versus α , Experimental and Calculated $M = 1.77$, $L/d = 7$, $R = 5.1 \times 10^6$	24

LIST OF FIGURES (CONCLUDED)

Figure	Title	Page
13	$C_{y,p}$ Versus α , Experimental and Calculated $M = 1.77$, $L/d = 5$, $R = 5.1 \times 10^6$	25
14	$C_{y,p}$ Versus α , Experimental and Calculated $M = 1.57$, $L/d = 7$, $R = \frac{566,000}{\text{Cal}}$	26
15	$C_{y,p}$ Versus α , Experimental and Calculated $M = .914$, $L/d = 7$, $R = 4.56 \times 10^6$	27
16	$C_{y,p}$ Versus α , Experimental and Calculated $M = .810$, $L/d = 7$, $R = 4.44 \times 10^6$	28
17	$C_{y,p}$ Versus α , Experimental and Calculated $M = .6$, $L/d = 7$, $R = 3.88 \times 10^6$	29
18	$C_{y,p}$ Versus α , Experimental and Calculated $M = .291$, $L/d = 7$, $R = 2.21 \times 10^6$	30
19	$C_{y,p}$ Versus α , Experimental and Calculated $M = .291$, $L/d = 7$, $R = 2.21 \times 10^6$	31
20	$C_{y,p}$ Versus α , Experimental and Calculated $U = 300 \text{ ft/sec}$, $L/d = 7$, $R = \frac{.77 \times 10^6}{\text{Cal}}$	32
21	$C_{y,p}$ Versus α , Experimental and Calculated $U = 300 \text{ ft/sec}$, $L/d = 7$, $R = \frac{.77 \times 10^6}{\text{Cal}}$	33
22	$C_{y,p}$ Versus α , Experimental and Calculated $U = 300 \text{ ft/sec}$, $L/d = 7$, $R = \frac{.77 \times 10^6}{\text{Cal}}$, RPM 4320.	34
23	$C_{y,p}$ Versus α , Experimental and Calculated $U = 300 \text{ ft/sec}$, $L/d = 7$, $R = \frac{.77 \times 10^6}{\text{Cal}}$, RPM 400	35

SYMBOLS

C_o	Crossflow correlation constant
C_l	Two dimensional lift coefficient lift per unit span/ $\frac{1}{2}\rho U_c^2 d$
$C_{y,p}$	Magnus force coefficient $8F_y/\rho U^2 \pi d^2 \bar{p}$
$C_{y,p\alpha}$	Slope of $C_{y,p}$, $\frac{\partial C_{y,p}}{\partial \alpha}$
F_y	Magnus force
L	Length of body
M	Mach number
R_o	Radius to the outer edge of the boundary layer
R	Reynolds number - based on length
R_c	Crossflow Reynolds number, $\frac{U_c d}{\nu}$
U	Freestream velocity
U_c	Crossflow velocity, $U \sin \alpha$
V_s	Surface velocity of body due to spin
d	Diameter of body
$f()$	Function of whatever is contained within the parenthesis
k	Constant of proportionality
$k(x)$	Axial circulation distribution
p	Pressure lb/ft ²
\bar{p}	Non-dimensionalized spin rate = $\frac{\omega d}{2U}$
r	Radial Coordinate, see Figure 1
r_o	Radius of the body
t	Time

u	Velocity in x-direction
v	Velocity in y-direction
w	Velocity in the ϕ -direction
x	Axial coordinate, see Figure 1
y	Coordinate, see Figure 1
z	Coordinate, see Figure 1
α	Angle of attack
δ	Boundary layer thickness
η	Transformed radial coordinate
μ	Coefficient of absolute viscosity
ν	Coefficient of kinematic viscosity
ξ	Transformed axial coordinate
ρ	Density
τ	Shear Stress
ω	Angular velocity, rad/sec
Γ	Circulation
Γ_0	Circulation based on surface velocity of the body
ϕ	Azimuthal Coordinate

Subscripts x, r, ϕ, η, ξ denote differentiation with respect to the subscript.

Subscripts 0, 1, 2, 3, 4, 5 denote the order of the approximation.

SECTION I

INTRODUCTION

When a sphere, cylinder, or other body of revolution which is moving through a fluid is rotated such that the axis of rotation is at an angle from its direction of translation, an aerodynamic force is produced. This force, called Magnus force, is in addition to lift or drag which may occur with or without spin. The direction of the Magnus force is perpendicular to the plane formed by the axis of rotation and the translation direction. The magnitude of this force is small when compared to the normal force which may be developed on a cylindrical body typical of a modern missile. It is found to be less than about 5 percent of this normal force. However, this force and its associated moment about the body center of gravity may be very important in predicting the flight path of spinning projectiles. For this reason it is of considerable interest to aerodynamicists and ballisticians. Although the Magnus effect has been observed for centuries and many measurements of its magnitude have been made, its origins have largely not been understood. It is the purpose of this report to review some of the theories that have been proposed to date and evaluate them as to their effectiveness in explaining and predicting the magnitude of this force.

SECTION II

HISTORICAL DISCUSSION

According to Swanson¹ the first record of the observation of the drift of a spinning body was made by G. T. Walker in 1671, the body was a sliced tennis ball. Later in 1730 B. Robins² expressed the opinion that the unexplained dispersion of cannon balls was due to the fact that they were spinning.

In order to try to put the ideas on a more firm footing, G. Magnus³ in 1852 performed some crude experiments both in the laboratory and in the field. He made measurements on a spinning cylinder with a flow normal to the axis of the cylinder and found that unequal pressures were developed on opposite sides of the cylinder due to the combination of the normal flow and the spin. In order to field test this on spheres, he fired musket balls which had the center of mass displaced from their geometric center. Then by placing the mass center to the right or left of the centerline of the musket, he could cause a spin to the right or left to develop. He found that in this way he could cause the musket ball to drift either to the left or right depending upon the direction of the spin. This demonstrated that the earlier ideas had been correct, and the phenomena came to be called the Magnus effect.

Lord Raleigh⁴, while studying the flight of a sliced tennis ball, was the first person to set up an ideal flow representation of the situation. He demonstrated that if one superimposes a uniform potential flow on a circulation a force in the proper direction will be produced. He noted, however, that his model was applicable only to a non-viscous fluid. His theory predicted no mechanism for the development of the needed circulation nor a relationship between the spin rate and magnitude of the force produced.

These results were followed by experiments by Lafay in Paris between 1910 and 1913^{5,6}. This work was done on spinning cylinders with a normal flow superimposed. Lift, drag, and pressure distributions were obtained for two different rotors at varying rotational speeds. One significant result of this study was the observation that at low spin rates a negative Magnus force was sometimes observed. This has been explained by Krahn³⁸ and is associated with the transition of the boundary layer from laminar to turbulent flow.

The dilemma of how the needed circulation could be developed was solved in 1918 when L. Prandtl⁷ showed that it could result

from boundary layer vorticity being shed by separation. The net vorticity of the shed boundary layer was equal and opposite to the resulting circulation. Recent studies by Buford⁸, Wood⁹ and Glauert¹⁰ show that the circulation imparted to the inviscid flow is always less than that of the circulation of the medium at the solid surface.

More experimental work was done by Reid¹¹, Thom¹²⁻¹⁷ and others through about 1935. Since that time many tests have been run on various configurations and a large body of data exist against which to compare any proposed theoretical solution to the problem. (See, for example, references 18 through 23.)

In more modern times a number of people have tried to give a solution for the problem. Examples of this may be seen in the work of Martin²⁴, Buford⁸, Swanson¹, Kelley²⁵, Kelley and Thacker²⁶, Platou²⁷, Iverson²⁸, Power²⁹, and others.

Generally, the theories try to relate the Magnus force at high angles of attack to the problem of normal flow over a spinning cylinder. In most cases of interest the boundary layer on such a cylinder will have separated, and the mechanism for the production of the circulation is as noted before. In the case of typical configuration at small angles a different mechanism is needed.

Martin's²⁴ work represents a step in the direction of trying to make predictions by the use of modern boundary layer theory. He analyzed the case for a spinning cylinder in incompressible laminar flow at small angle of attack. He obtained a solution for the three-dimensional boundary layer by the method of perturbations. With this he determined the displacement thickness of the boundary layer and used this new effective shape of the body to calculate, by slender body theory, the resultant Magnus force. This same approach was followed by Kelley²⁵ and Kelley and Thacker²⁶ who extend Martin's²⁴ work to higher spin rates and included a radial pressure gradient and skin friction effects. These theories predict a linear function of angle of attack. Experiments show that the force is not linear with angle of attack even at low angles and shows strong non-linearity at cross-flow Reynolds numbers lower than where one would expect to find separation. Further, experiments by Cowen and Perkins³⁰ and Dunn³¹ indicate that for non-spinning bodies with large L/D and at low angles of attack the normal force due to crossflow develops with distance down the body much the same as the flow develops about an impulsively-translated circular cylinder. Kelley's³² work on the prediction of the normal force on a non-spinning cylinder at an angle of attack used this approach.

Platou²⁷ suggests then that perhaps the Magnus force could be treated in an analogous manner. Platou further suggests that the normal velocity for each section of such a spinning body be taken as the component of the freestream velocity normal to the body axis. Further, the Magnus force on each section would be related, not to the steady state Magnus forces on a cylinder, but rather to the force on a rotating cylinder, impulsively rotated from rest before it has developed the steady-state force.

A numerical analysis of an impulsively rotated cylinder immersed in a uniform freestream was performed by Thoman and Szewczyk³³. From this work the cylinder force coefficient can be obtained as a function of time. Power and Iverson^{28,29} used Platou's²⁷ suggestion and the results of Thoman and Szewczyk³³ to predict the variation of the Magnus force with angle of attack and spin. The results predict the non-linearity with angle of attack, but the final equation contains a correlation constant which must be determined from experiment and which seems to take on a large range of values.

SECTION III

PROPOSED THEORIES

In this section several theories will be discussed that have been proposed to explain the Magnus force on a cylindrical spinning body which is inclined at a small angle α from the freestream. The boundary layer will be assumed to be laminar, and no provision is made for nose shape. Basically, all of these theories derive from the work of Martin²⁴ who was the first person to successfully apply modern boundary layer theory to this problem. Martin reasoned that in the small angle-of-attack region the Magnus force would not be due to circulation but rather to a distortion of the effective shape of the body due to the asymmetric boundary layer which would develop due to the spin. If this shape could be calculated, potential flow methods could be used to determine the force. Martin's first paper on this subject was in a cartesian coordinate system which has not turned out to be the simplest one to use for this case. In addition, there were some errors in the development. For these reasons the work of Kelley^{25,26} is used to show the basic methods for this solution of the problem. Kelley introduced the cylindrical coordinate system as shown in Figure 1.

The Navier-Stokes equations for steady state incompressible flow in the coordinate system shown in Figure 1 are:

$$(ru)_x + (rv)_r + w_\phi = 0 \quad (1)$$

$$uu_x + vu_r + \frac{w}{r}u_\phi = -\frac{1}{\rho}p_x + \nu \nabla^2 u \quad (2)$$

$$uv_x + vv_r + \frac{w}{r}v_\phi - \frac{w^2}{r} = -\frac{1}{\rho}p_r + \nu [V^2 v - \frac{v}{r^2} - \frac{2}{r^2}w_\phi] \quad (3)$$

$$uw_x + vw_r + \frac{w}{r}w_\phi + \frac{vw}{r} = -\frac{1}{\rho}p_\phi + \nu [V^2 w + \frac{2}{r^2}v_\phi - \frac{w}{r^2}] , \quad (4)$$

where u and v are the velocities in the x and y directions and w is the velocity in the ϕ direction and subscripts denote partial differentiation.

As is customary in Boundary Layer Theory, the above equations are nondimensionalized and by an order-of-magnitude argument they are reduced to the boundary layer equations. (For details of this reduction, see reference 25.) The non-dimensional boundary

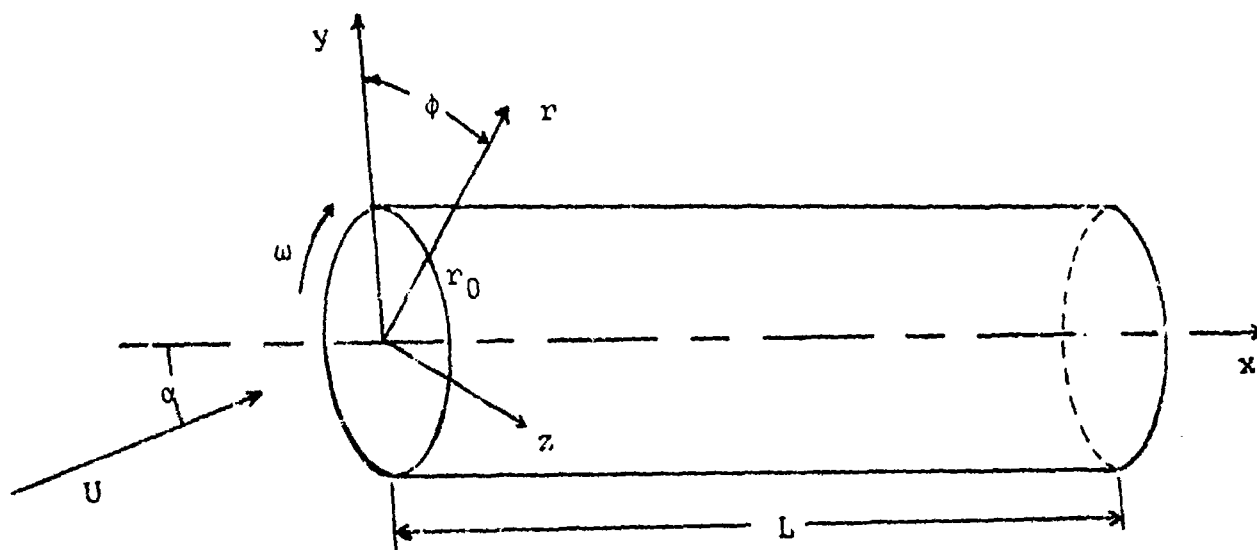


Figure 1. Coordinate System

layer equations for flow over a cylinder, as shown in Figure 1, may be written:

$$(ru)_x + (rv)_r + w_\phi = 0 \quad (5)$$

$$uu_x + vu_r + \frac{w}{r} \phi = \frac{v}{r} (ru_r)_r \quad (6)$$

$$uw_x + vw_r + \frac{w}{r} w_\phi + \frac{vw}{r} = -\frac{1}{\rho r} p_\phi + \frac{v}{r} (rw_r)_r \quad (7)$$

$$uv_x + vv_r + \frac{w}{r} v_\phi - \frac{w^2}{r} = -\frac{1}{\rho} p_r + \frac{v}{r} (rv_r)_r \quad (8)$$

In the above equations terms to order $\frac{\delta^2}{r_0}$ have been retained and higher order terms have been neglected. The first three of these are used to calculate the velocity profiles while the last is used to calculate a correction due to the radial pressure gradient after u , v , and w are determined.

Next it was assumed that the velocity components could be expressed in the form

$$\frac{u}{U} = u_0 + u_1 + u_2 + u_3 + u_4 + u_5 + u_6$$

$$\frac{v}{U} = v_0 + v_1 + v_2 + v_3 + v_4 + v_5 + v_6$$

$$\frac{w}{U} = w_1 + w_2 + w_3 + w_4 + w_5 + w_6$$

where u_0 and v_0 are non-dimensional velocity components for zero spin and zero angle of attack. The subscript 1 refers to terms linear in α or ω , and subscript 2 denotes terms of order α^2 , $\alpha\omega$, ω^2 , and so on for the other subscripts.

To zero order the above equations reduce to

$$(ru_0)_x + (rv_0)_r = 0 \quad (9)$$

$$u_0 u_{0x} + v_0 u_{0r} = \frac{u}{U} (ru_{0r})_r \quad (10)$$

Equation (4) vanishes since for $\alpha = \omega = 0$, $w = 0$ and the derivative with respect to ϕ also vanishes. Using numerical integration techniques, Seban and Bond³⁴ solved the two remaining equations by making the transformations

$$\xi = \frac{4}{r_0} \sqrt{\frac{vx}{U}} \quad (11)$$

$$\eta = \frac{r^2 - r_0^2}{4r_0} \sqrt{\frac{U}{vx}} \quad (12)$$

The solution may be written

$$u_0 = \frac{f_\eta}{2} \quad (13)$$

$$v_0 = \frac{r_0}{2r} \sqrt{\frac{U}{vx}} (\eta f_\eta - f - \xi f_\xi) \quad (14)$$

These satisfy equation (9) identically and allow equation (10) to be written

$$[(1+\eta\xi)f_{\eta\eta}]_{\eta} + ff_{\eta\eta} + \xi[f_{\xi}f_{\eta\eta} - f_{\eta}f_{\eta\xi}] = 0. \quad (15)$$

This can be reduced to a system of ordinary differential equations by assuming $f(\eta, \xi)$ to be a polynomial in ξ :

$$f(\eta, \xi) = f_0(\eta) + f_1(\eta)\xi + f_2(\eta)\xi^2 + \dots \quad (16)$$

and terminating this after the first order terms. Using this reduces equation (15) to three third-order ordinary differential equations with boundary conditions such that

$$u = v = 0, \quad w = r\omega \quad \text{at } r_0 \quad (17)$$

$$u = U(1 - \frac{\alpha^2}{2}) \quad (18)$$

$$w = U\alpha \sin\phi(1 + \frac{R_0}{r^2}) \quad \text{for large } r. \quad (19)$$

The Navier-Stokes equations are rewritten six times, each time considering terms of one higher order of perturbation. Details of this calculation as well as the profiles of u , v , and w are presented in reference 26.

Once u , v , and w were known, it was possible to calculate how far a streamline at the outer edge of the boundary layer would be moved outward from the position it would have had in a frictionless fluid. That is the displacement thickness. The method for doing this was worked out by Dunn and Kelley³⁵ and was done in detail by Kelly and Thacker²⁶. This gave an effective shape induced by the spin such as shown in Figure 2.

Slender body potential flow theory was applied to this, and a force coefficient was obtained in terms of the profile functions. This result is included in equation (21).

In the normal thin boundary layer theory it is customary to assume that there is no pressure gradient normal to the solid surface. This assumption is not good in this case. Equation (8) shows that a non-zero value for $\frac{\partial p}{\partial r}$ will be obtained. This equation to order $\frac{\delta}{L}$ will yield

$$\frac{1}{\rho} \frac{\partial p}{\partial r} = \frac{w^2}{r}. \quad (20)$$

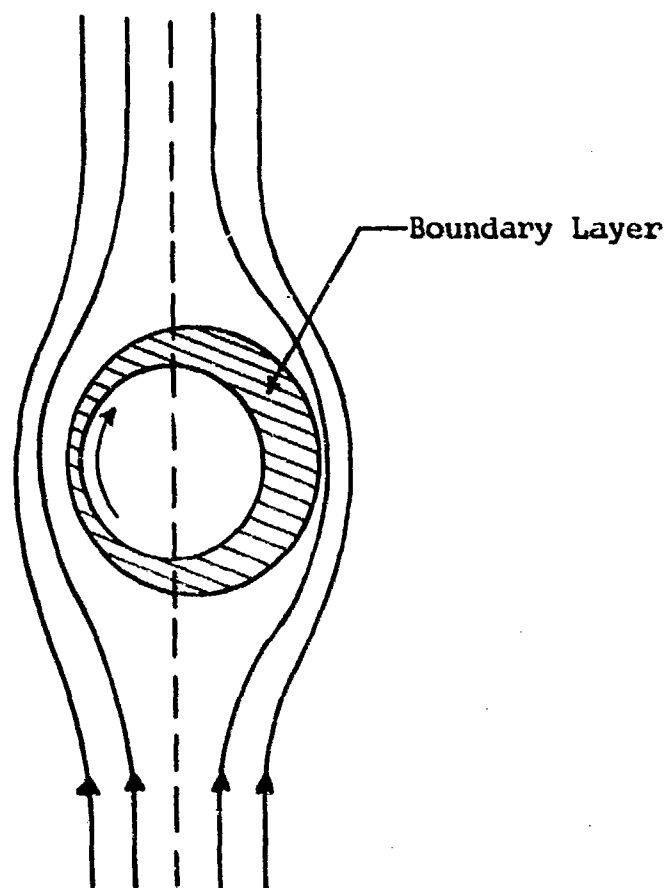


Figure 2. Effective Shape

Using this relationship and the w profile functions, Kelley and Thacker²⁶ obtained a second order term in the Magnus force due to this radial pressure gradient.

As is well known, the skin friction shear stress at a solid boundary such as this problem presents is given by Newton's relationship

$$\tau = \mu \left. \frac{\partial w}{\partial r} \right|_{r=r_0}$$

If this is integrated over an area, a skin friction force is obtained. Taking the y component, this can be shown to be

$$F_y = \int_0^{2\pi} r_0 \tau \cos \phi d\phi \quad \text{per unit length.}$$

Since the gradient $\frac{\partial w}{\partial r}$ is not a constant around the circumference, a net side force results. Using the profile functions, Kelley and Thacker²⁶ obtained a third order contribution to the Magnus force from this mechanism.

Combining the effect of displacement thickness, radial pressure gradient, and skin friction, they found

$$C_{y,Pa} = \frac{8}{\sqrt{R}} \left(\frac{L}{d} \right)^2 [7.834 - 16.526 \left(\frac{L}{d} \right)^2 \left(\frac{r_0 \omega}{U} \right)^2 + \dots] \quad (21)$$

This result is compared with a number of experimental measurements in Figures 3 through 23.

As could be expected, due to the assumptions made in the derivation, this equation does not give good results above very small angles. In an effort to rectify this situation, Iverson²⁸ and Power and Iverson²⁹ have modified this scheme to account for the non-linearity that has been found.

All of the previous work has assumed that no circulation was present in the inviscid outer flow since there was no separation of the boundary layer. It is known, however, from work on non-spinning slender bodies that at fairly small angles of attack, about six degrees, body vortices may be formed. It seems quite plausible then to assume that an axial distribution of circulation may be induced. Power and Iverson²⁹ assumed that this circulation could be approximated by assuming that the cross-flow along the x-axis of the spinning cylinder at low angles of attack is similar to the unsteady flow over an impulsively rotated cylinder placed perpendicular to the free-stream. The boundary conditions at the outer edge of the boundary layer were assumed to be:

$$u = U(1 - \frac{\alpha^2}{2}) \quad (22)$$

$$w = U \sin \phi \left(1 + \frac{R_0^2}{r^2} \right) + \frac{k(x) \Gamma_0}{2\pi r} \quad (23)$$

where $\Gamma_0 = 2\pi r_0 v_\theta$ and $k(x) = \frac{\Gamma}{\Gamma_0}$ and

where Γ is the circulation that actually exists. Note that these boundary conditions differ from the ones previously used only by the term representing the shed vorticity. Values of $k(x)$ were found by using the results of Thoman and Szewczyk³³. Power²⁹ found that for an impulsively rotated cylinder in a crossflow the force coefficient was well represented for small time by

$$C_1 = \frac{U_c t}{d} \left(\frac{v_s}{U_c} \right) \sqrt{\frac{U_c d}{v}} \quad (24)$$

To apply this to the spinning cylinder crossflow let

$$U_c = U \sin \alpha \quad (25)$$

$$t = \frac{x}{U \cos \alpha} \quad (26)$$

$$\frac{v_s}{U_c} = \frac{\bar{p}}{\sin \alpha} \quad (27)$$

The local circulation strength is given by

$$\Gamma = \frac{1}{2} C_1 U_c d \quad (28)$$

Using equations (24) and (28) one can write

$$k(x) = \frac{\Gamma}{\Gamma_0} = \frac{C_0}{2\pi} \left(\frac{x}{d} \right) \tan \alpha \sqrt{\frac{U_c d}{v}} \quad (29)$$

which reduces for small α to

$$k(x) = \frac{C_0}{128\pi} R_c^{-1/2} \xi^2$$

C_0 is a crossflow correlation constant to be determined from experiment and R_c is a crossflow Reynolds number.

With these new conditions Power²⁹ solved the boundary layer equations in a manner similar to that used by Kelley²⁵. After the velocity profiles were obtained, contributions to the Magnus force by displacement thickness, radial pressure gradient, skin friction, and circulation distribution were

obtained. The final result is given by

$$C_{y,p} = \frac{q}{\sqrt{R}} \left(\frac{L}{d} \right)^2 \left\{ 60.97 + (.637 R_c^{.75} C_o - 357.37) \left(\frac{L}{d} \right) \frac{1}{\sqrt{R}} - \frac{227.01}{R} \left(\frac{L}{d} \right)^2 \right\} \quad (30)$$

Results from the use of this equation are compared with experimental test results in Figures 17, 18, and 22.

Iverson²⁸ took an approach to the problem that is based on the same basic idea as the work described above. Instead of going through a boundary layer calculation he took a phenomenological approach and tried to find a correlation parameter directly from experimental results. He used equations (25) through (27) repeated below

$$U_c = U \sin \alpha \quad (25)$$

$$t = \frac{x}{U \cos \alpha} \quad (26)$$

$$\frac{v_s}{U_c} = \frac{F}{\sin \alpha} \quad (27)$$

and equation (24) in the form

$$C_1 = f \left\{ \frac{U_c t}{d} \left(\frac{v_s}{U_c} \right) \left(\frac{U_c d}{v} \right)^{-\frac{1}{4}} \right\}.$$

Putting these together it is possible to obtain

$$C_1 = f \left\{ \frac{x}{d} \frac{\tan \alpha}{\sin^{5/4} \alpha} \left(\frac{U d}{v} \right)^{-\frac{1}{4}} \right\} \quad (31)$$

This is a local side force coefficient based on the projected side-area and the cross-flow dynamic pressure. In order to get it for the complete body, simply integrate from 0 to L and change the reference area to $\pi d^2/4$ and the dynamic pressure to free-stream to obtain

$$C_{y,p} = k \frac{2}{\pi} \left(\frac{L}{d} \right)^2 \tan \alpha \sin^{3/4} \alpha \left(\frac{U d}{v} \right)^{-\frac{1}{4}} \quad (32)$$

Iverson²⁶ then plotted the Magnus force coefficient versus

$$\frac{2}{\pi} \left(\frac{L}{d} \right)^2 \tan \alpha \sin^{3/4} \alpha \left(\frac{Ud}{v} \right)^{-1/4}$$

for a number of experimental cases. He was thus able to find k which according to the theory should be a constant good for many cases. A summary of results based on this equation is given in the Section IV.

SECTION IV

RESULTS

The theories outlined in the previous section are compared with experimental results of a number of investigators working in many different tunnels. All of the models were slender, pointed bodies of revolution with no boattailing. Details as to Mach number, spin rate, and such are given on the figures.

The theory that has been commonly used to predict the Magnus coefficient for slender bodies of revolution at low angles of attack is that of Kelley²⁵. The result, obtained before the work with Thacker²⁶, was the same as equation (21) except that it did not contain the higher order term for spin. The result is given by

$$C_{y,pa} = \frac{62.672}{\sqrt{R}} \left(\frac{L}{d} \right)^2 . \quad (33)$$

It is found that the coefficient does decrease with spin rate but not at the rate predicted by equation (21). Equation (33) then has proven to be more accurate than the higher order one. For that reason the results presented in the following figures uses equation (33).

The results of the work by Power and Iverson²⁹ are represented by equation (30) and is shown for comparison on Figures 17, 18, and 22. The value of C_0 that was used is shown on each figure.

Equation (32) represents the semi-empirical result obtained by Iverson²⁸. He found, on looking at experimental data, that k took on values from 5 to 20. Since k is a constant of proportionality, the $C_{y,p}$ values predicted could be different by as much as a factor of 4. In this study a large amount of experimental data was examined in order to find a reasonable value of k . It has long been observed that the Magnus force increased with spin rate in a more or less linear fashion for low spin rates. At higher spin rates there is a change in the slope of the curve. Since equation (32) contains no provision for accounting for this non-linearity, only wind tunnel data in this spin range was examined in this attempt to evaluate k . Based on these restrictions, a value of $k = 10$ was selected. The results for this are shown in Figures 3 through 23.

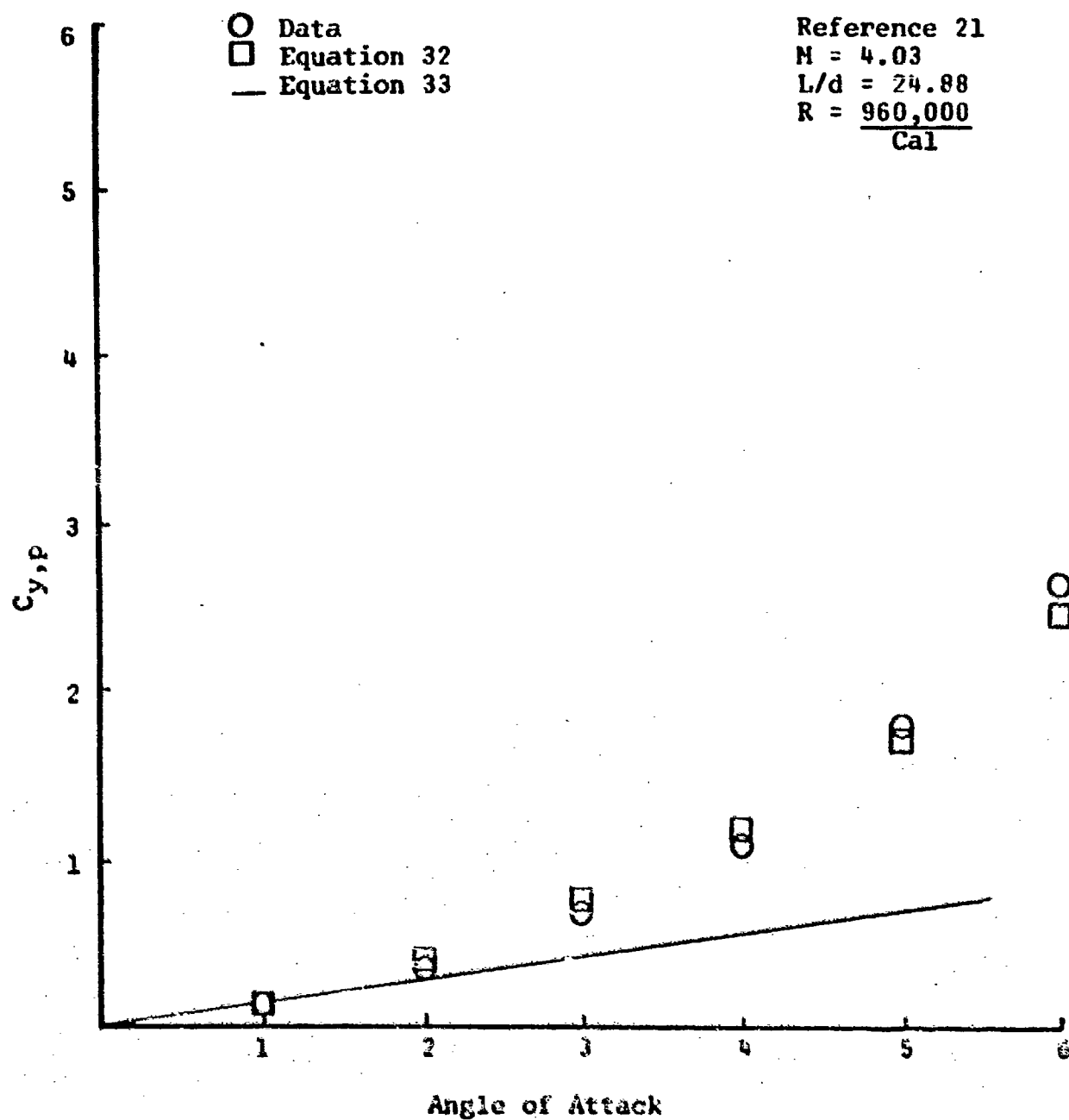


Figure 3. $C_{y,p}$ Versus α , Experimental and Calculated $M = 4.03$,
 $L/d = 24.88$, $R = \frac{960,000}{Cal}$

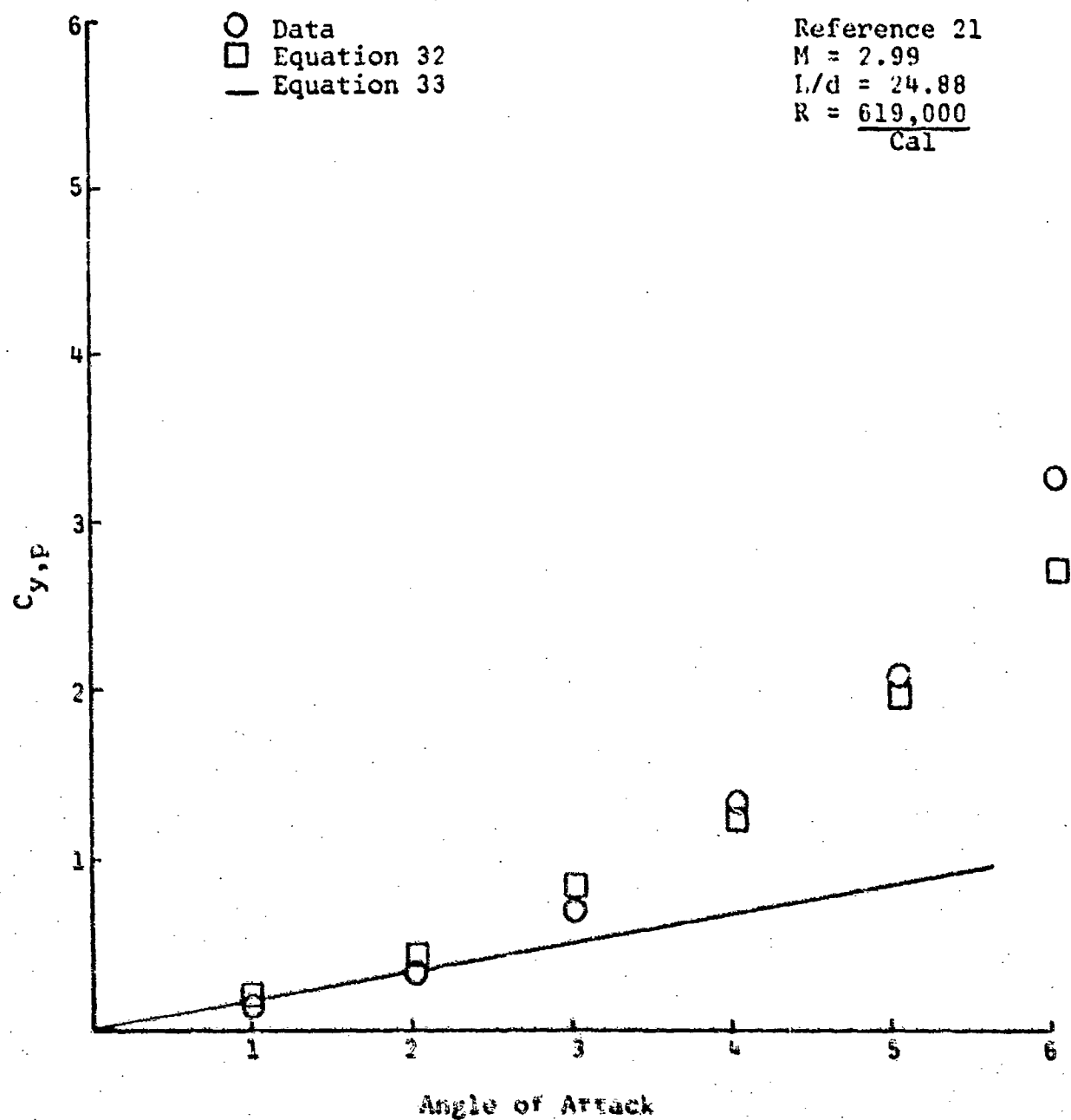


Figure 4. $C_{y,p}$ Versus α , Experimental and Calculated $M = 2.99$,
 $L/d = 24.88$, $R = \frac{619,000}{Cal}$

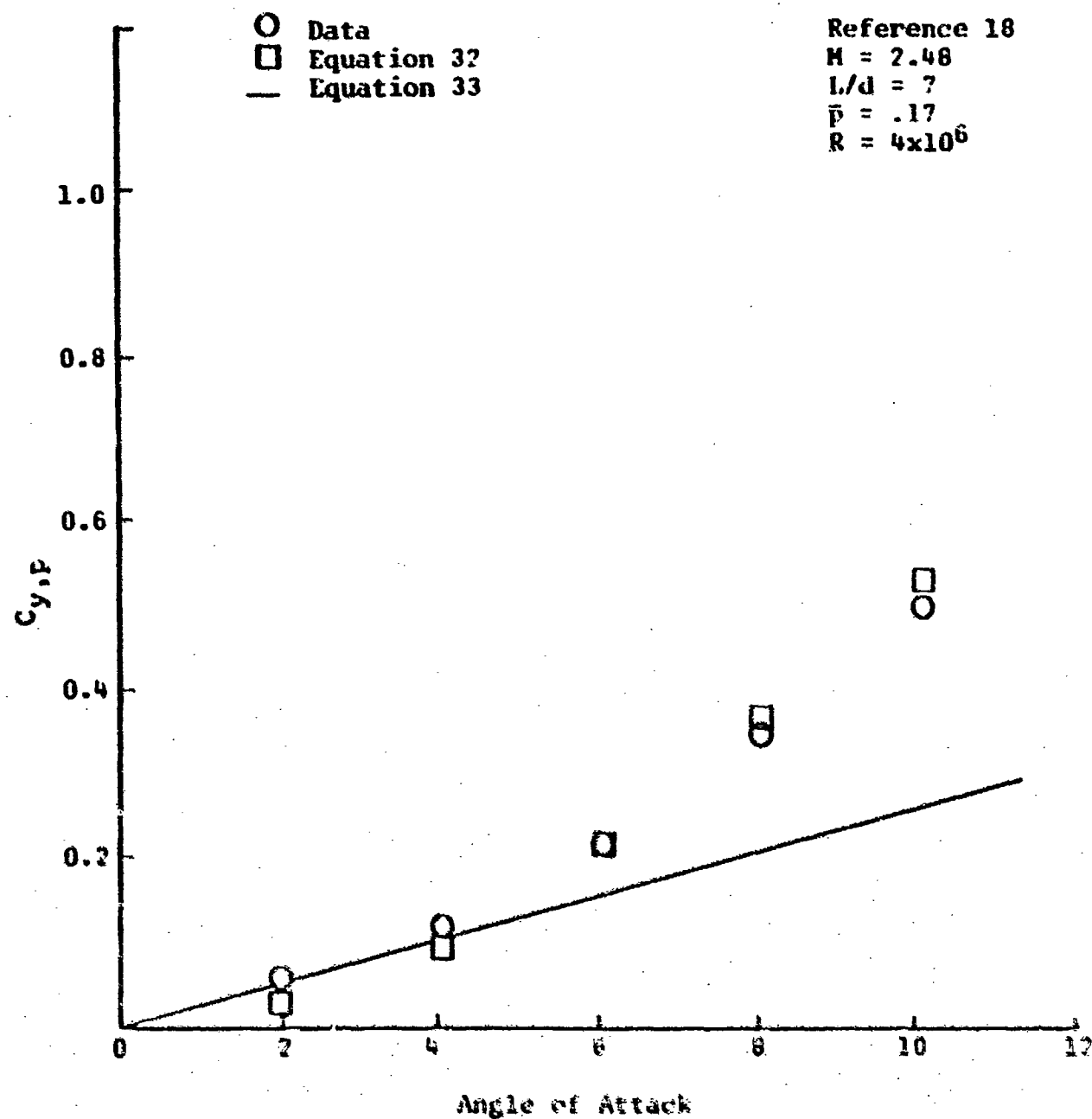


Figure 5. $C_{y,p}$ Versus α , Experimental and Calculated $M = 2.48$,
 $L/d = 7$, $R = 4 \times 10^6$

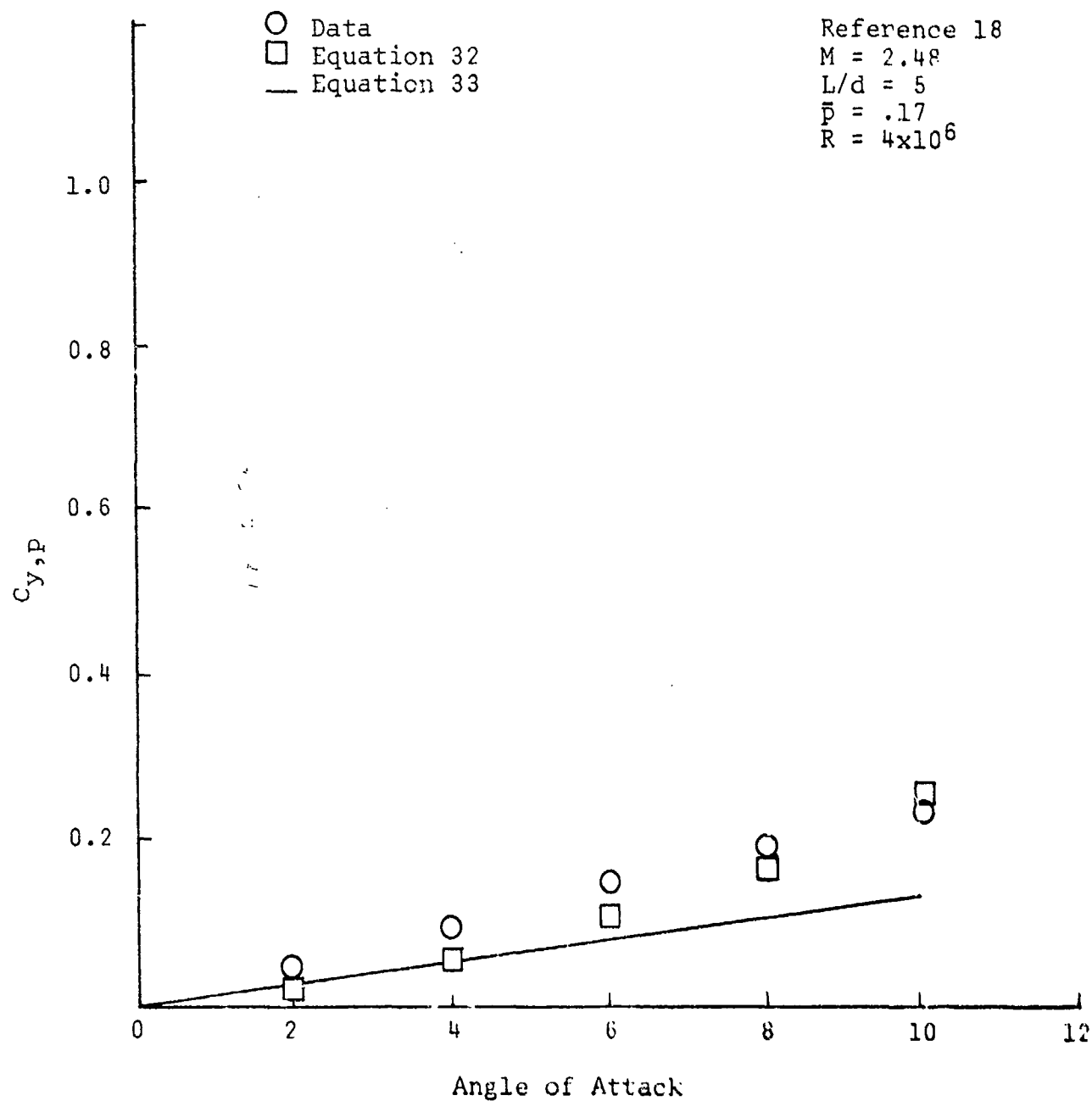


Figure 6. $C_{y,p}$ Versus α , Experimental and Calculated $M = 2.48$,
 $L/d = 5$, $R = 4 \times 10^6$

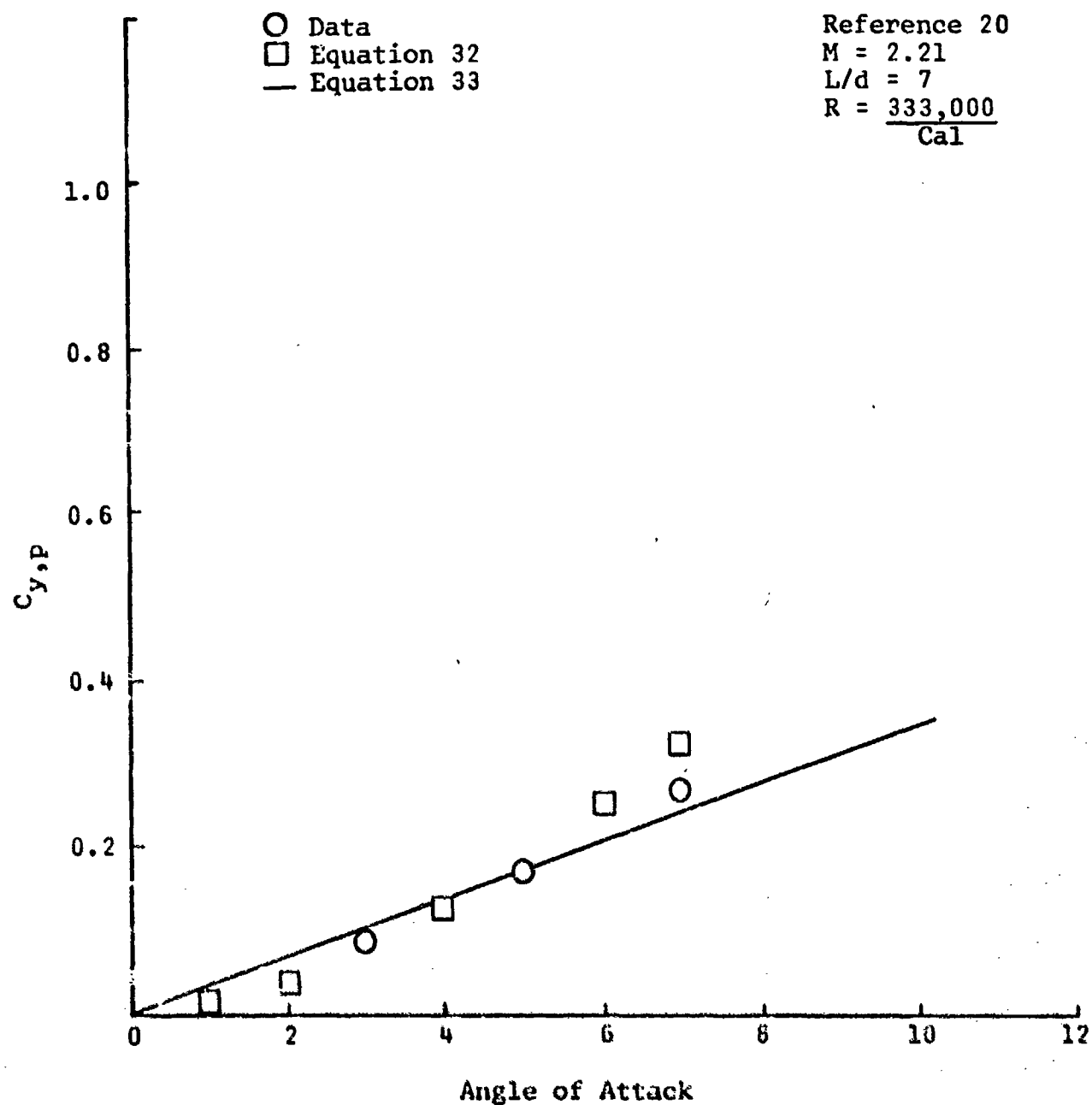


Figure 7. $C_{y,p}$ Versus α , Experimental and Calculated $M = 2.21$,
 $L/d = 7$, $R = \frac{333,000}{Cal}$

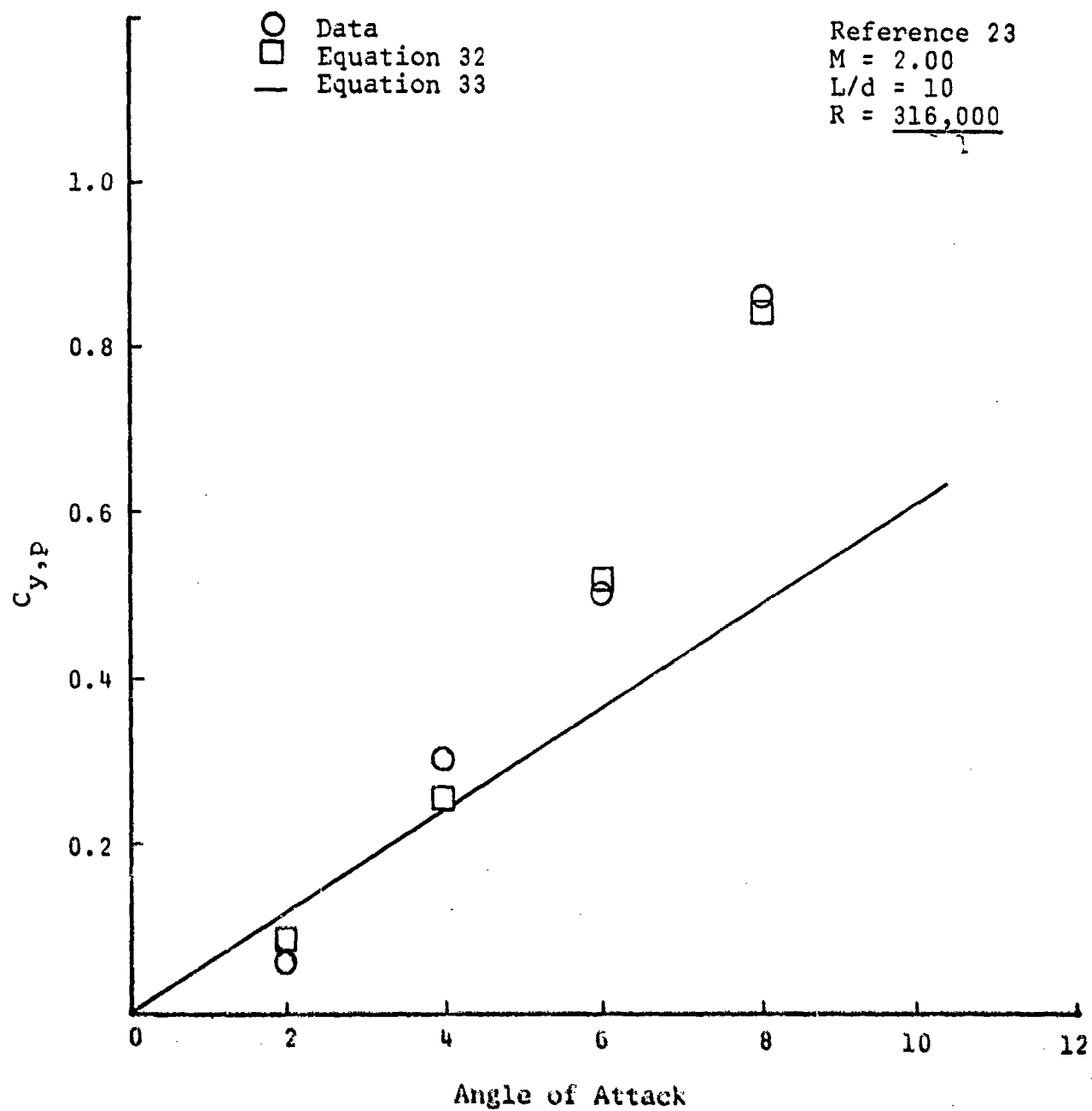


Figure 8. $C_{y,p}$ Versus α , Experimental and Calculated $M = 2.00$,
 $L/d = 10$, $R = \frac{316,000}{Cal}$

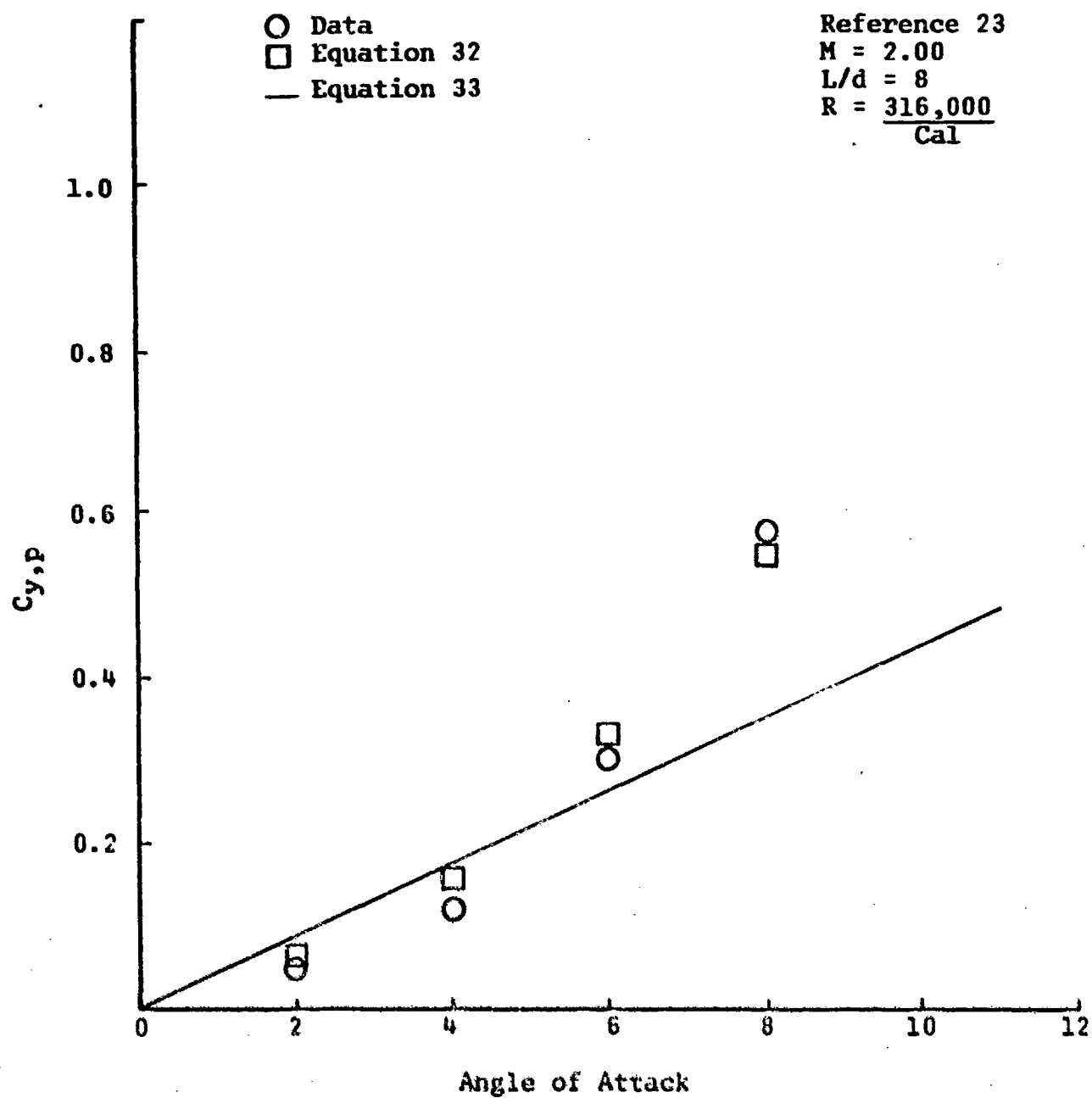


Figure 9. $C_{y,p}$ Versus α , Experimental and Calculated $M = 2.00$,
 $L/d = 8$, $R = \frac{316,000}{Cal}$

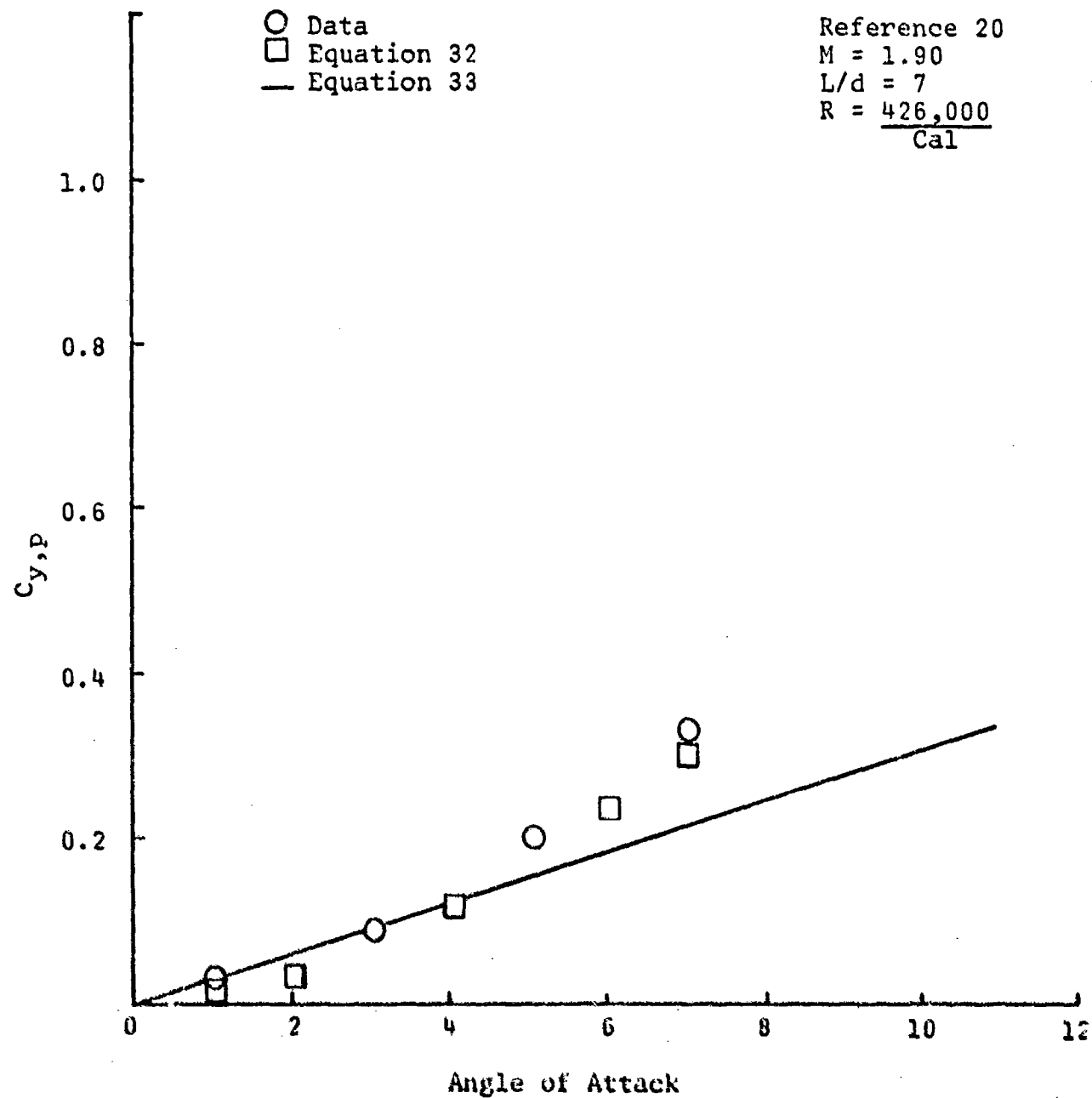


Figure 10. $C_{y,p}$ Versus α , Experimental and Calculated $M = 1.90$,
 $L/d = 7$, $R = \frac{426,000}{\text{Cal}}$

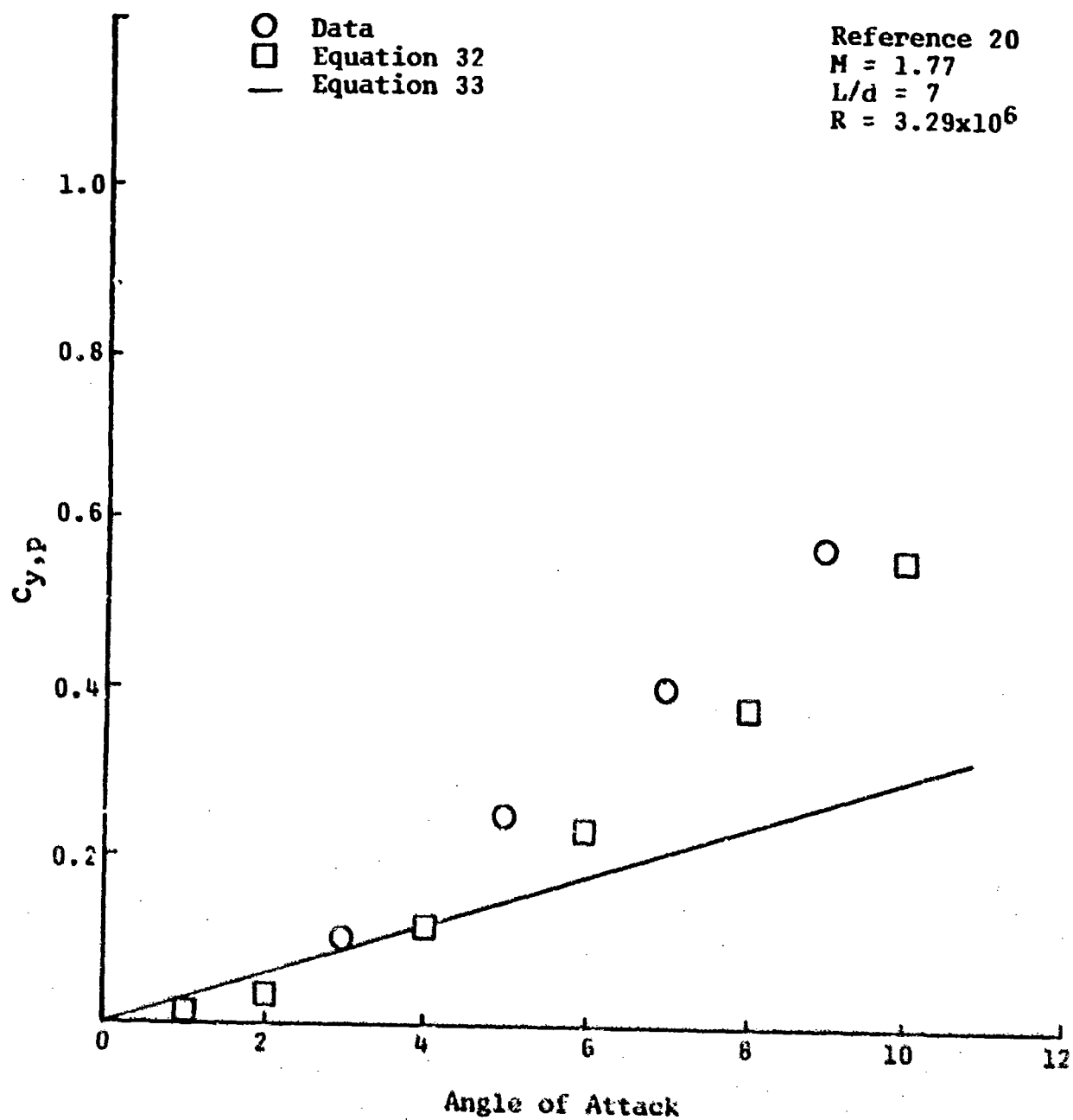


Figure 11. $C_{y,p}$ Versus α , Experimental and Calculated $M = 1.77$, $L/d = 7$, $R = 3.29 \times 10^6$

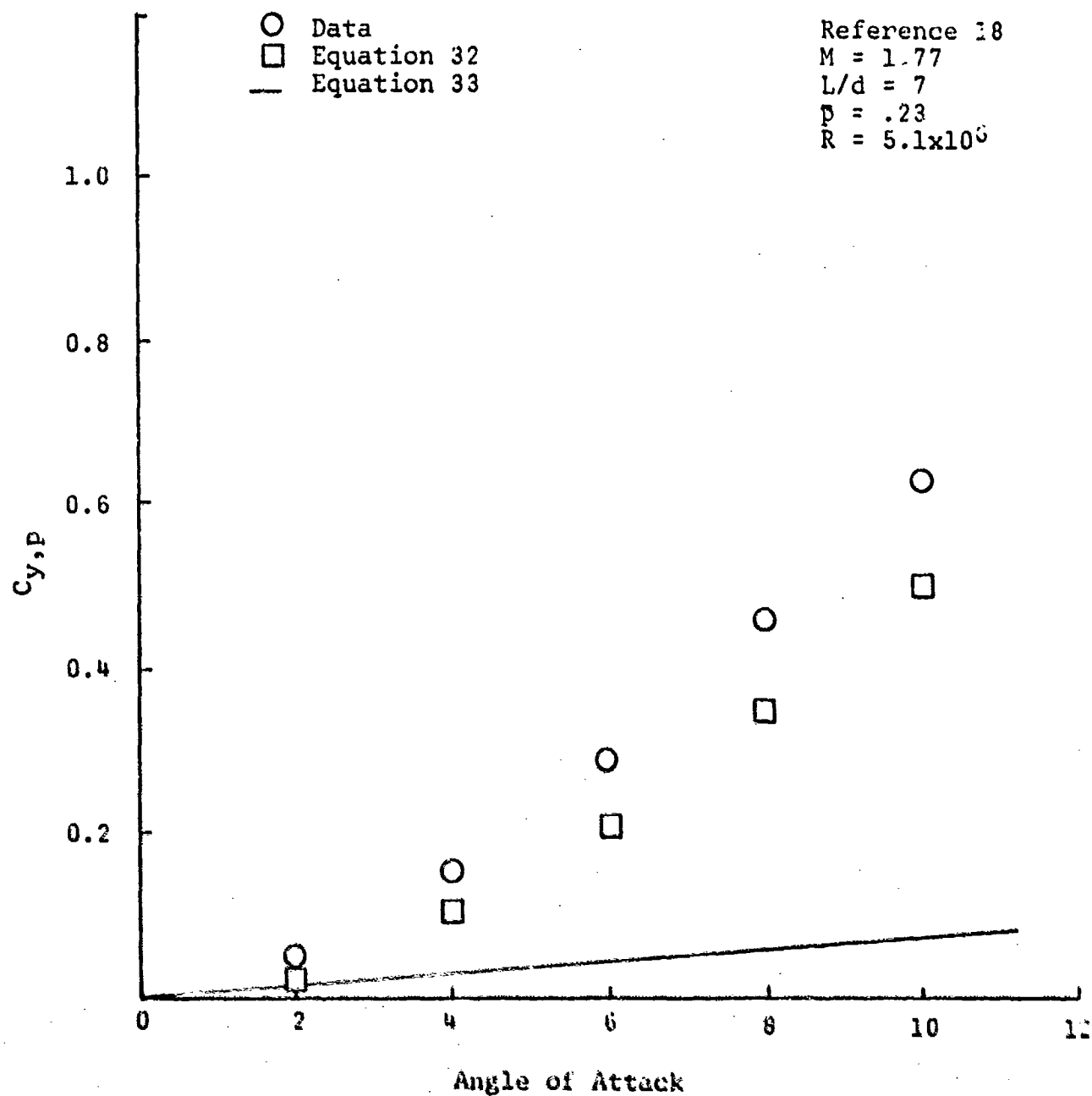


Figure 12. $C_{y,p}$ Versus α , Experimental and Calculated $M = 1.77$,
 $L/d = 7$, $R = 5.1 \times 10^6$

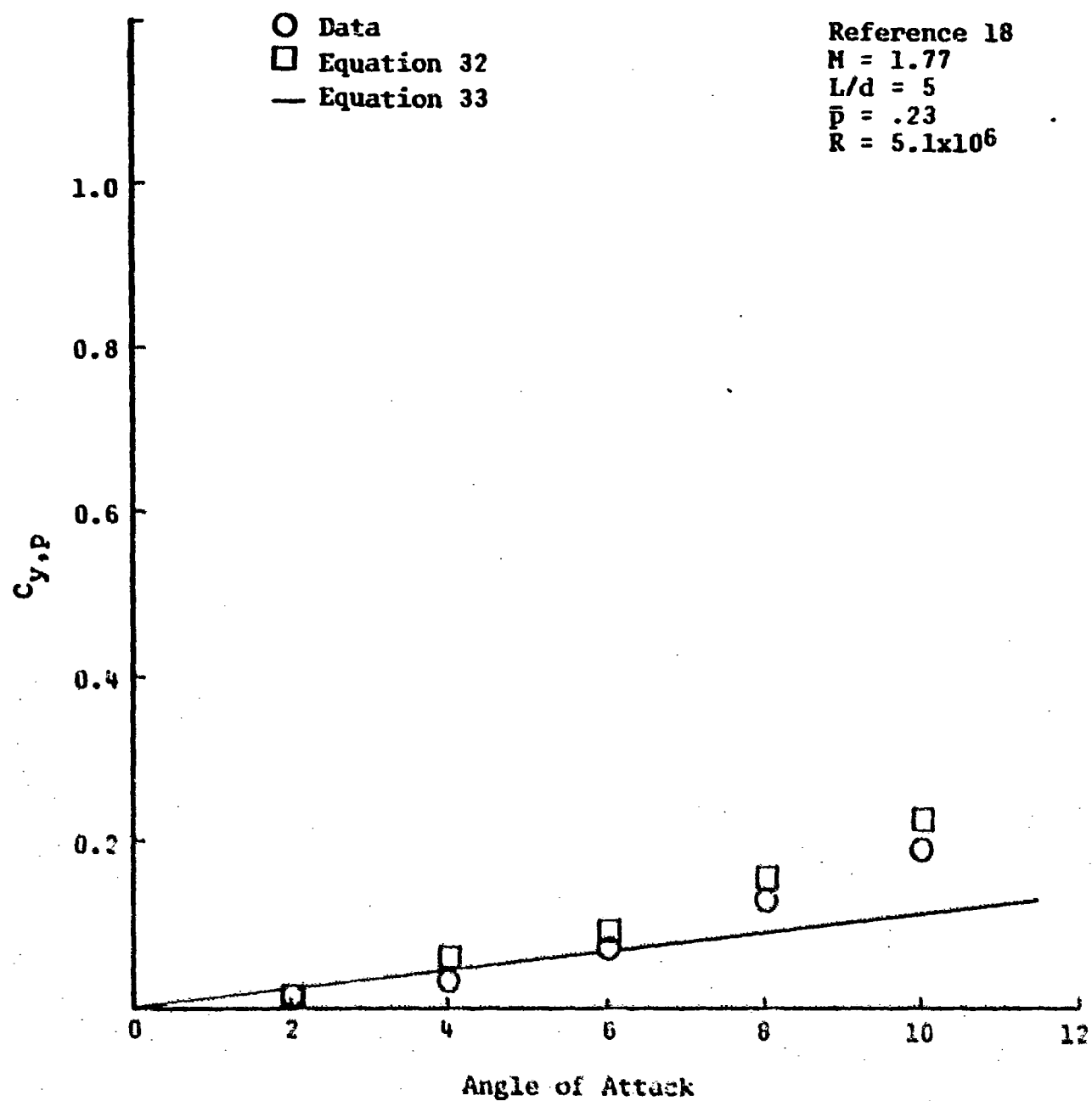


Figure 13. $C_{y,p}$ Versus α , Experimental and Calculated $M = 1.77$,
 $L/d = 5$, $R = 5.1 \times 10^6$

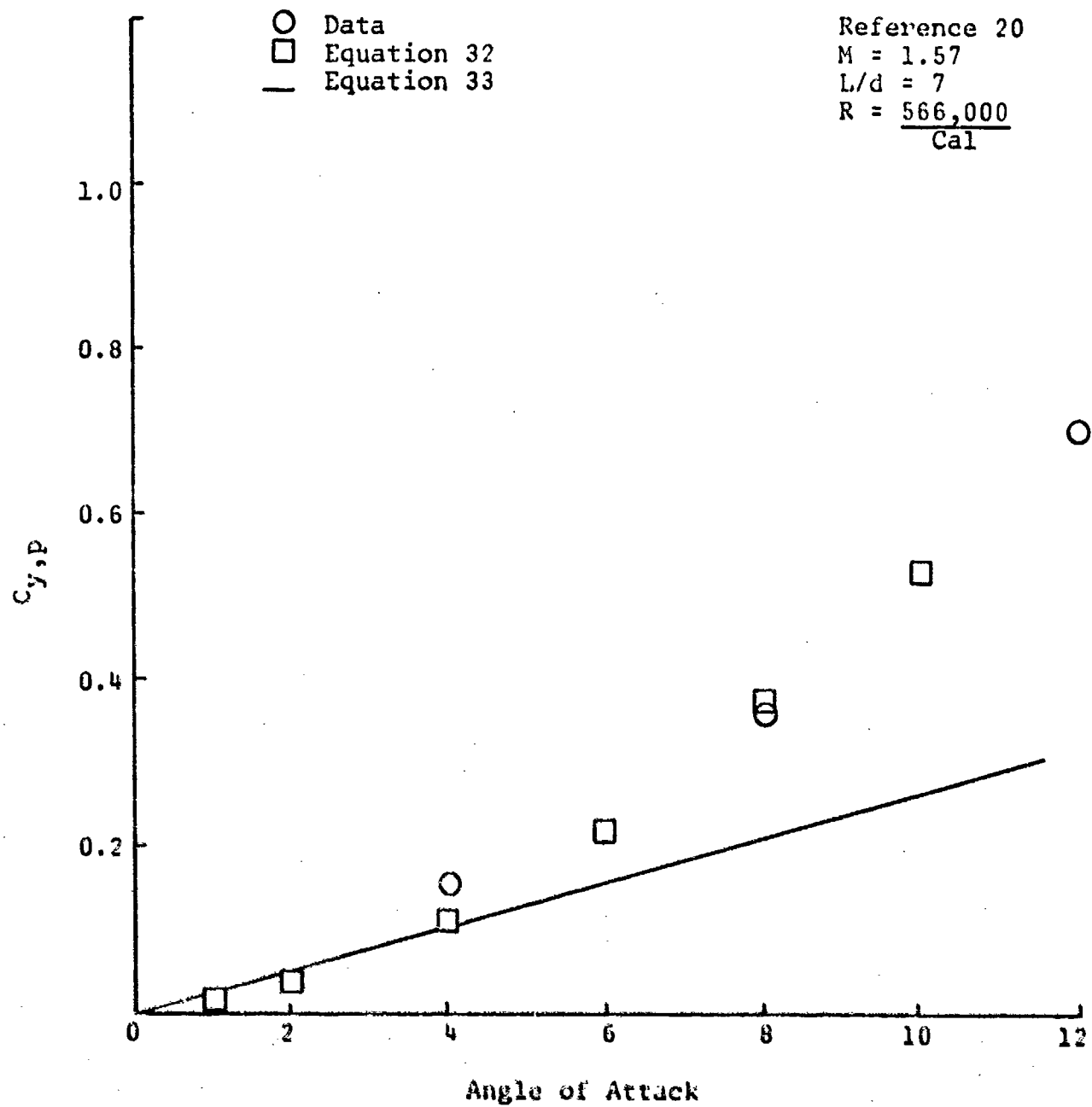


Figure 14. $C_{y,p}$ Versus α , Experimental and Calculated $M = 1.57$,
 $L/d = 7$, $k = \frac{566,000}{\text{Cal}}$

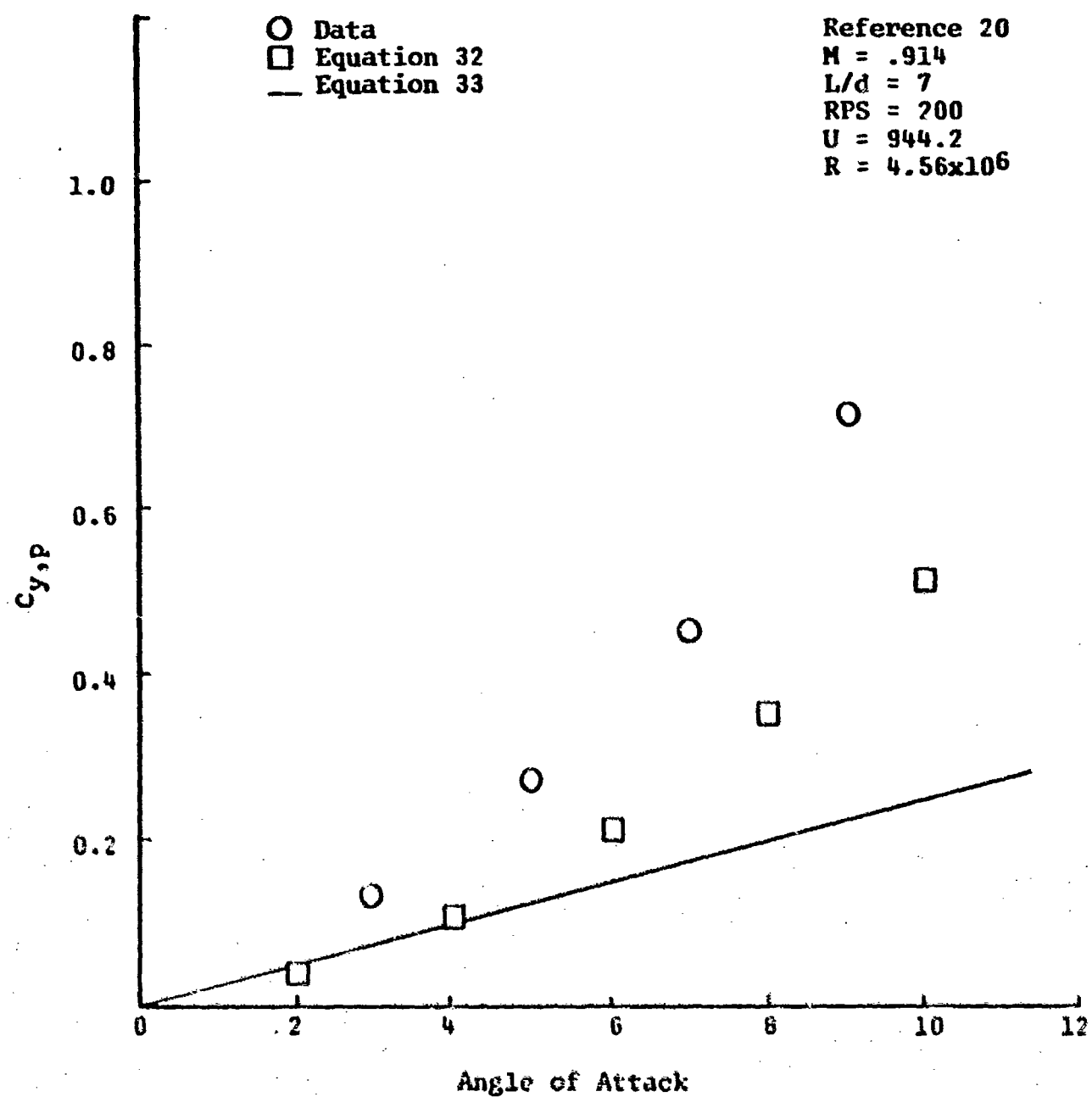


Figure 15. $C_{y,p}$ Versus α , Experimental and Calculated $M = .914$,
 $L/d = 7$, $R = 4.56 \times 10^6$

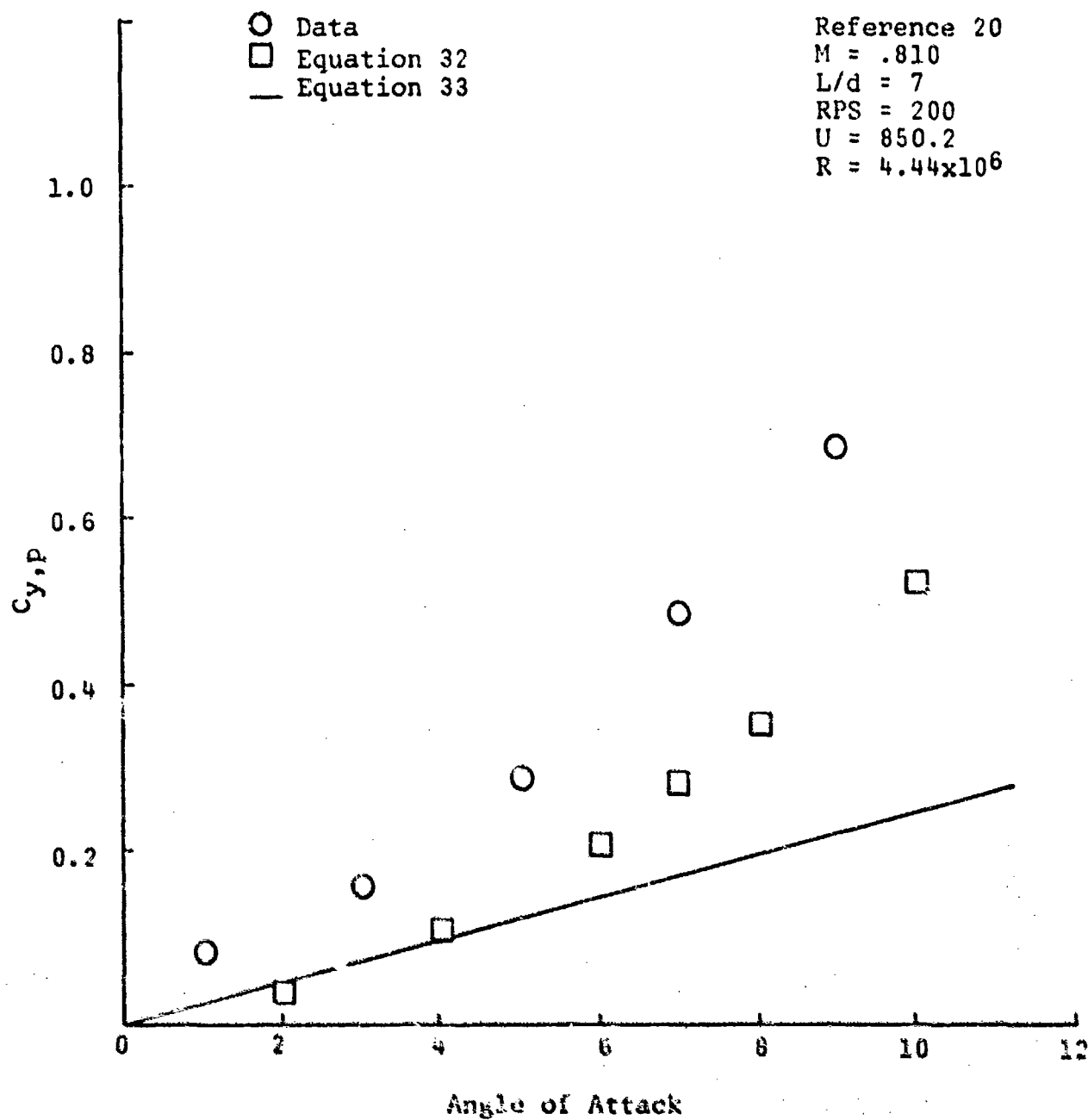


Figure 16. $C_{y,p}$ Versus α , Experimental and Calculated $M = .810$,
 $L/d = 7$, $R = 4.44 \times 10^6$

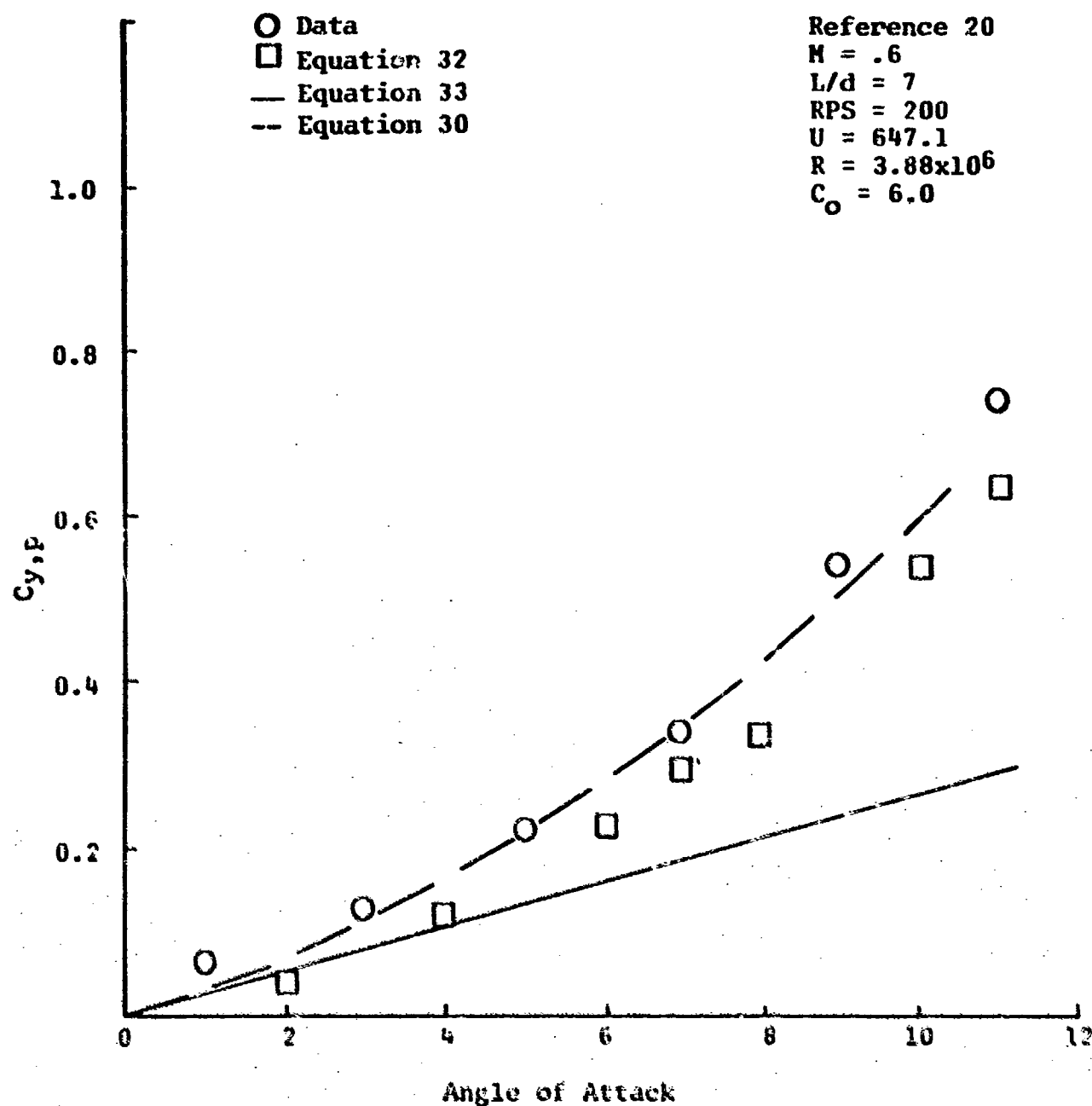


Figure 17. $C_{y,p}$ Versus α , Experimental and Calculated $M = .6$,
 $L/d = 7$, $R = 3.89 \times 10^6$

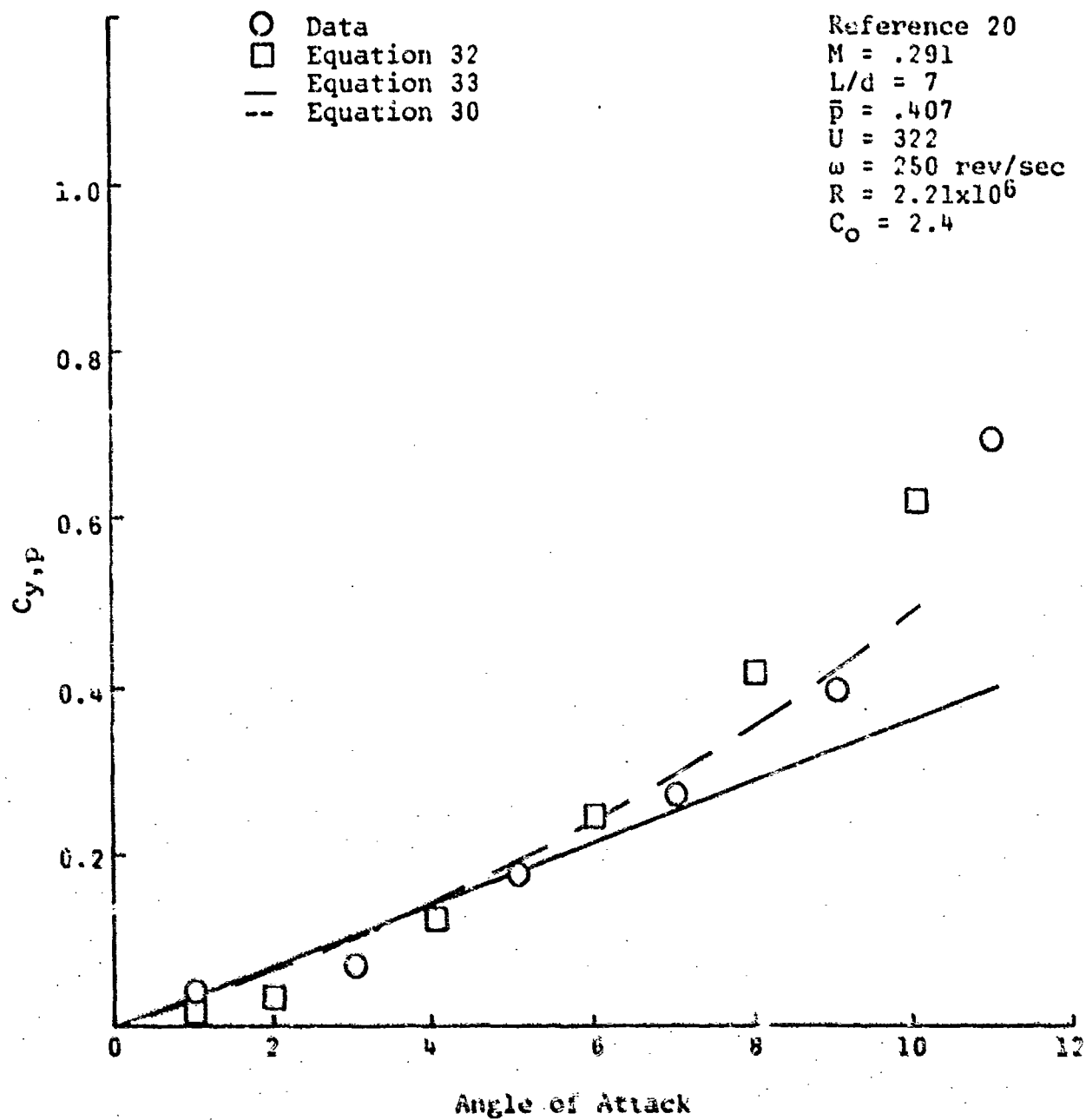


Figure 18. $C_{y,p}$ Versus α , Experimental and Calculated $M = .291$,
 $L/D = 7$, $R = 2.21 \times 10^6$

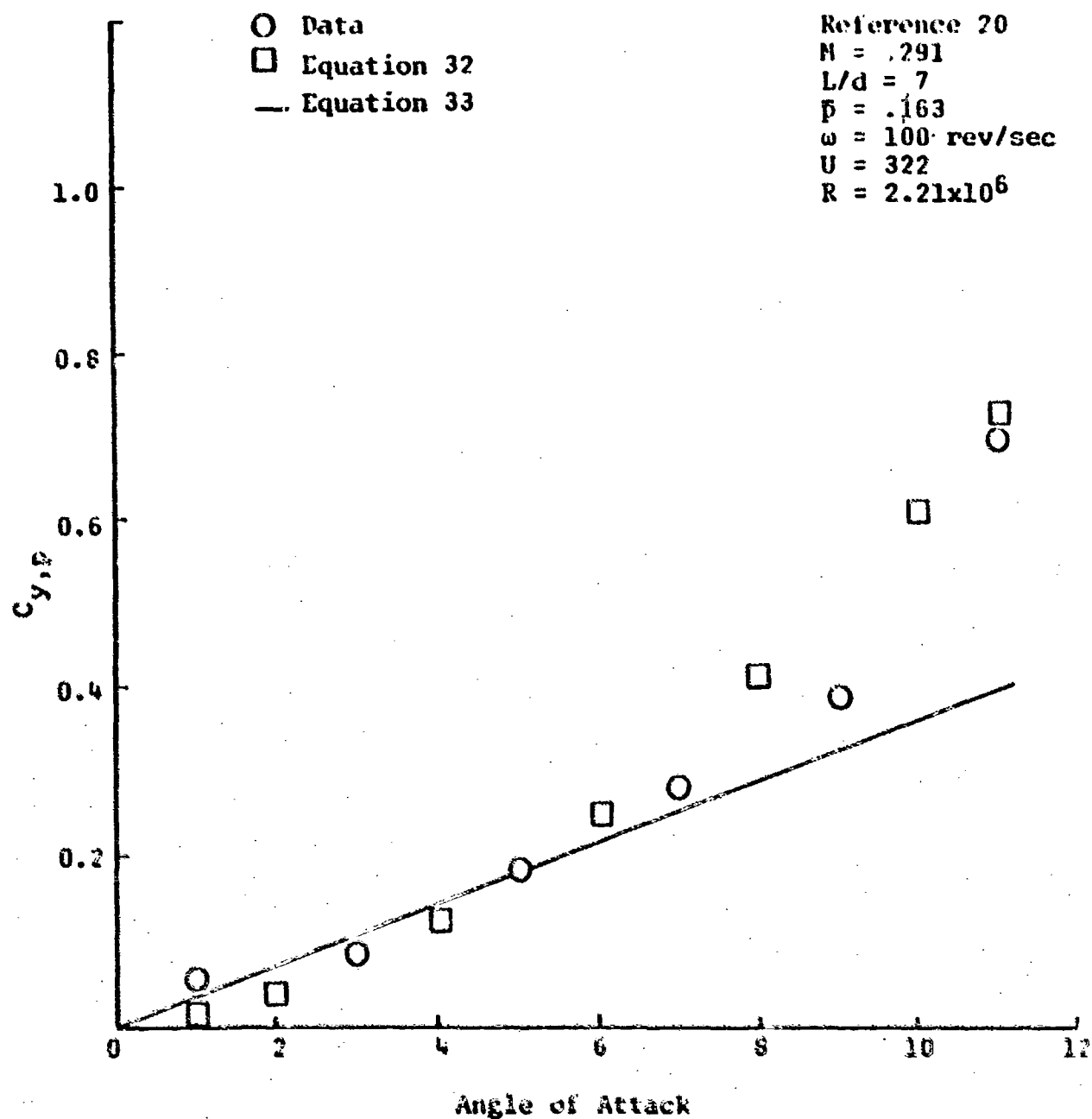


Figure 19. $C_{y,p}$ Versus α , Experimental and Calculated $M = .291$,
 $L/d = 7$, $R = 2.21 \times 10^6$

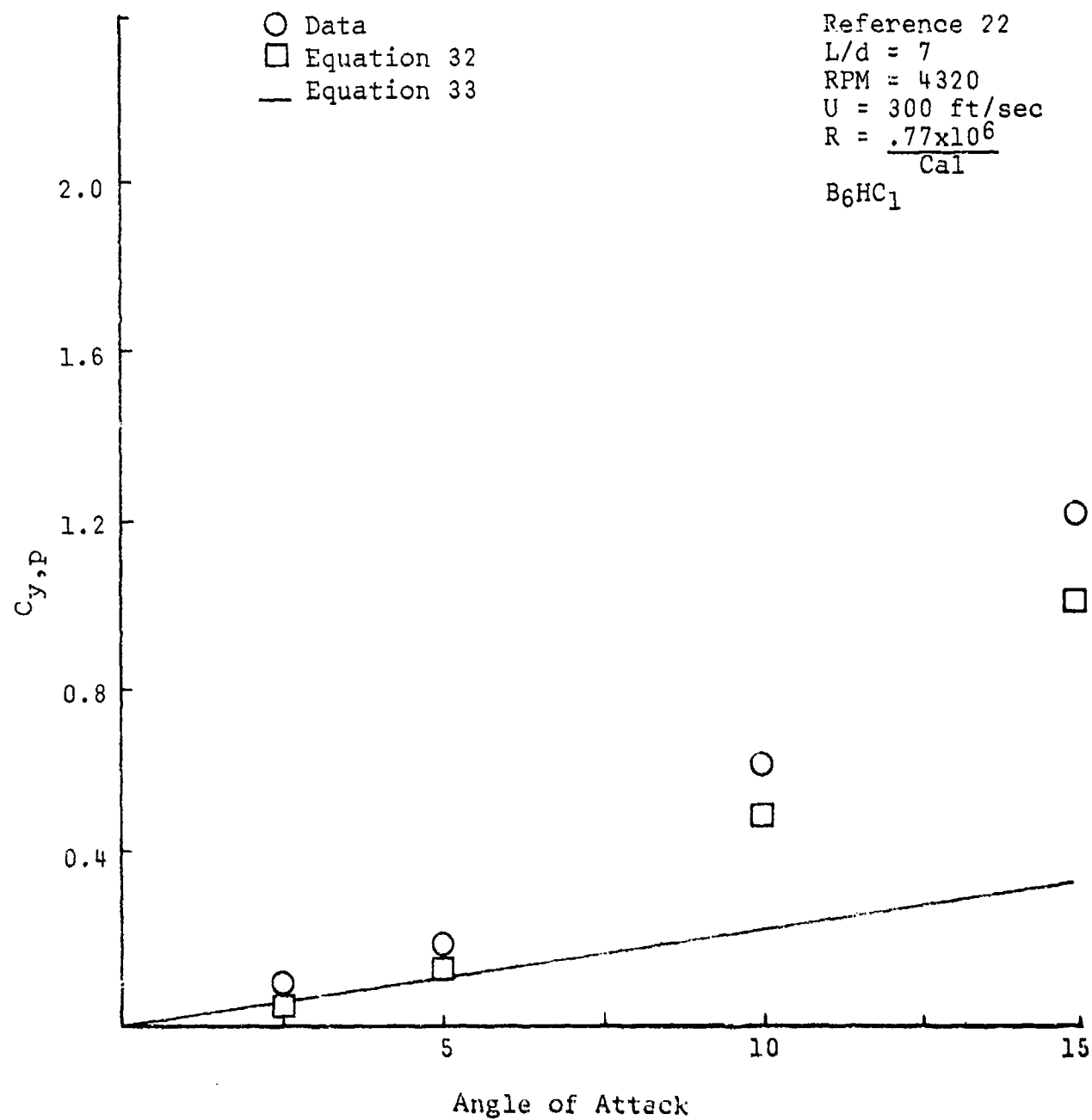


Figure 20. $C_{y,p}$ Versus α , Experimental and Calculated

$U = 300 \text{ ft/sec}$, $L/d = 7$, $R = \frac{.77 \times 10^6}{Cal}$

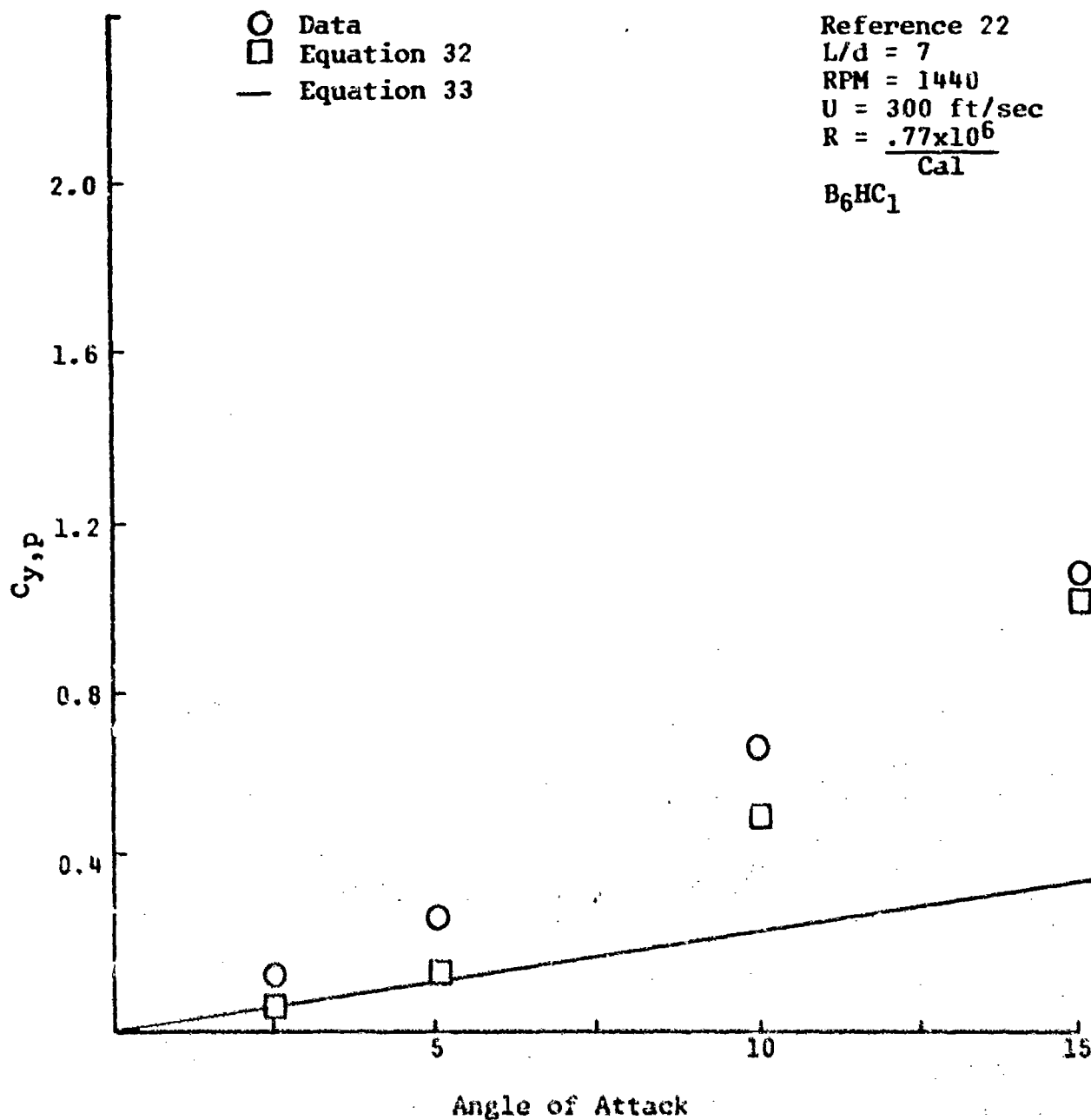


Figure 21. $C_{y,p}$ Versus α , Experimental and Calculated

$U = 300 \text{ ft/sec}$, $L/d = 7$, $R = \frac{.77 \times 10^6}{Cal}$

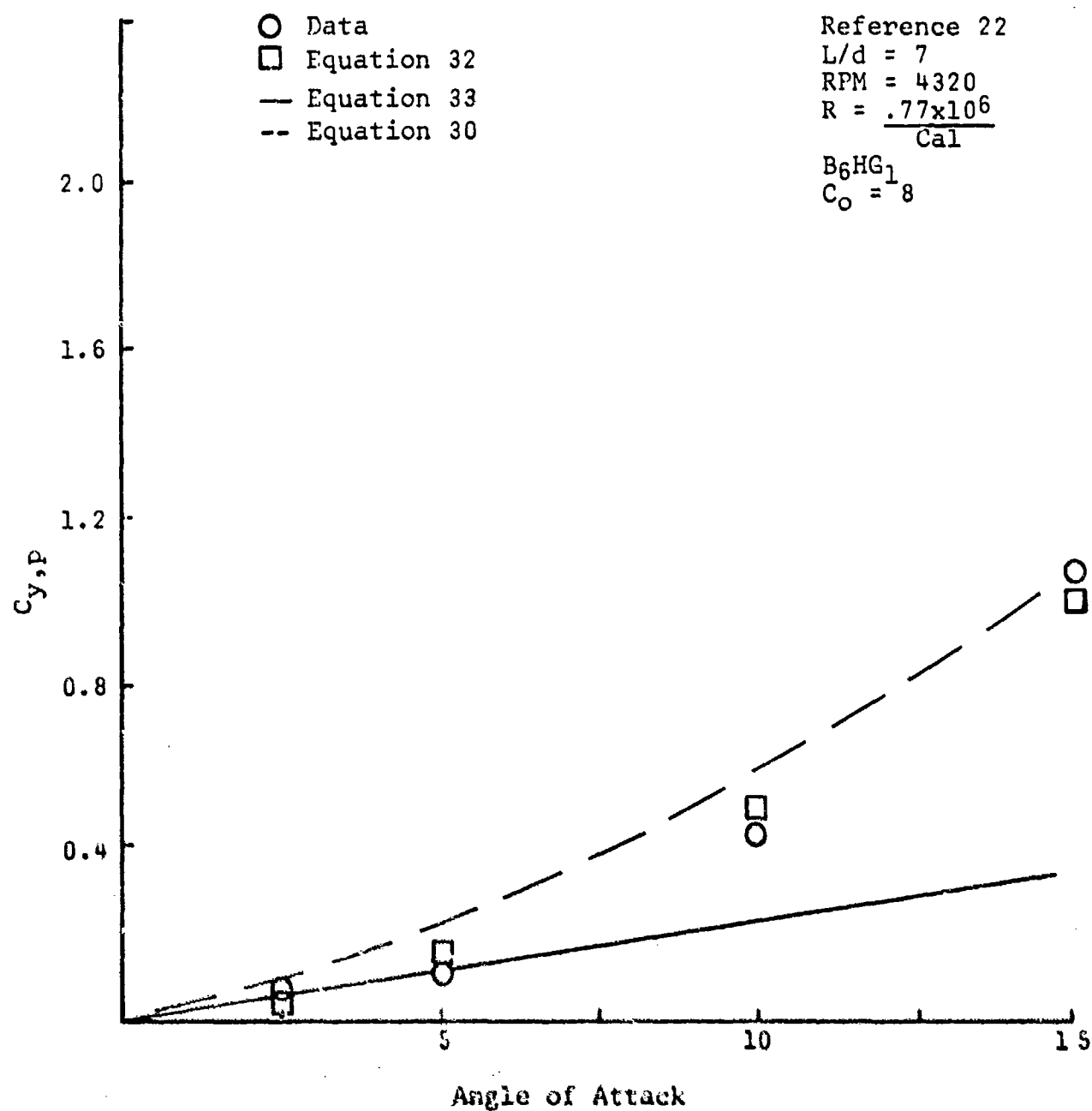


Figure 22. $C_{y,p}$ Versus α , Experimental and Calculated

$U = 300$ ft/sec, $L/d = 7$, $R = \frac{.77 \times 10^6}{Cal}$, RPM 4320

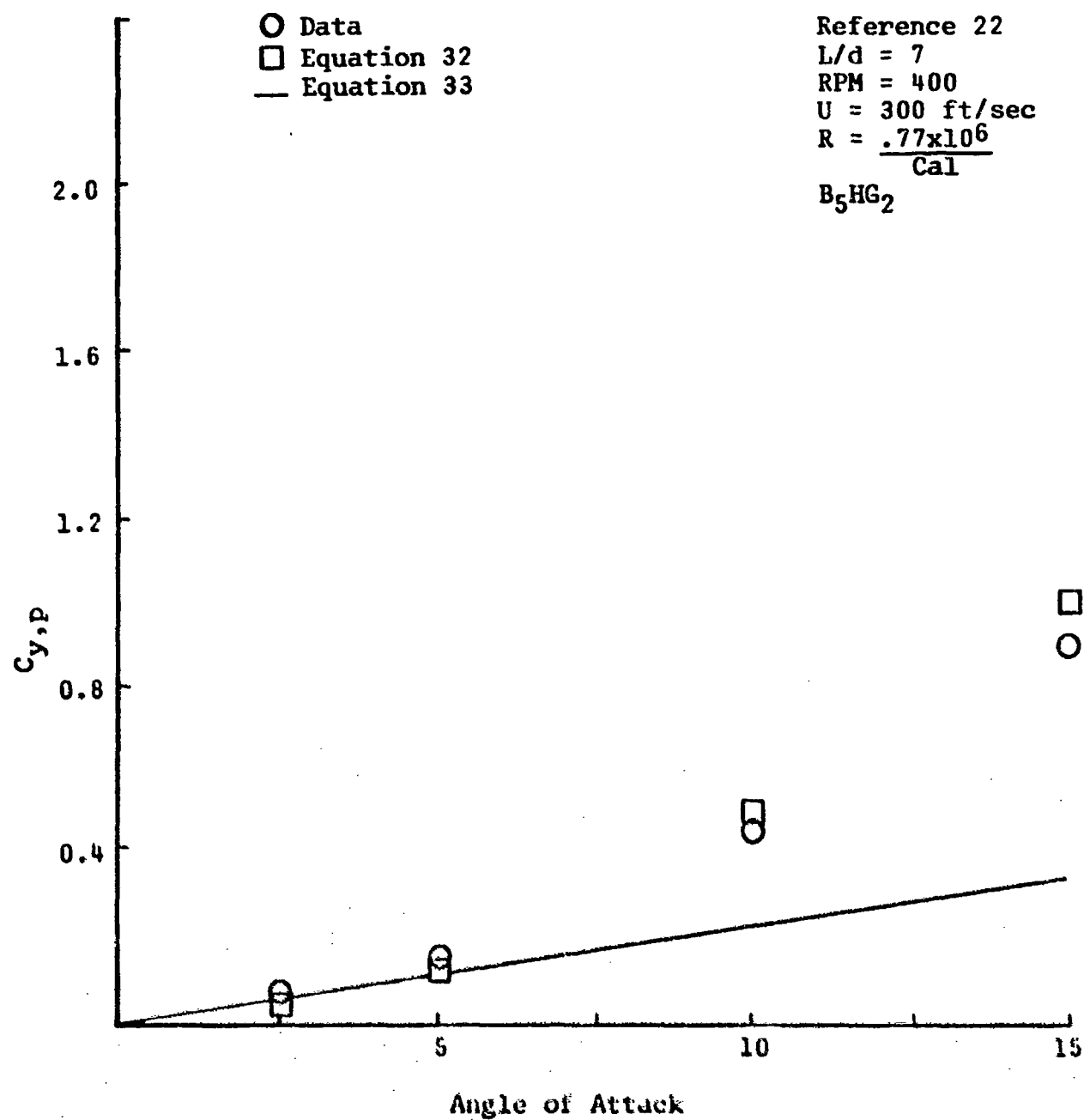


Figure 23. $C_{y,p}$ Versus α , Experimental and Calculated

$U = 300 \text{ ft/sec}$, $L/d = 7$, $R = \frac{.77 \times 10^6}{Cal}$, $RPM = 400$

SECTION V

DISCUSSION AND CONCLUSIONS

As is obvious from Figures 3 to 23, equation (33) gives reasonable results only in the case of very small angles of attack. This is not surprising since it was derived for a laminar boundary layer in incompressible flow with no separation. The works of Martin²⁴, Kelley and Thacker^{25,26} were an attempt to solve the problem from first principles and were intended to be the forerunner for theoretical work on more practical cases. Unfortunately the mathematics involved is so complex that these much needed improvements have yet to appear. Indeed it will be necessary to calculate the boundary layer separation lines on a spinning inclined body of revolution in order to get the solution from first principles. Some idea of the magnitude of the problem may be obtained by realizing that the state of the art is such that this information is only beginning to be available for non-spinning bodies. These results are still open to serious question and, in fact, the definition of what constitutes separation of a three-dimensional boundary layer is still under debate³⁶.

For these reasons Power and Iverson²⁹ have taken a semi-empirical approach based on suggestions²⁷ that the problem could be treated in a manner similar to methods used to predict the non-linear variation of forces on non-spinning bodies.

Power's result, equation (30), does give the proper shape of the $C_{y,p}$ versus α curves as seen in Figures 17, 18, and 22. It was necessary to use values of 2.4 to 8 for C_0 in order to make the equation fit the data in just these three cases. Neither Power nor this author has been able to obtain C_0 in a systematic way and until this can be done equation (30) will not be useful in predicting the Magnus force.

Equation (32) with $k = 10$ does give reasonable answers for most of the cases studied in this report. There does seem to be a systematic error that develops in the transonic region. This is not surprising since the prediction of any aerodynamic characteristic in this region is difficult. Care should be taken in the application of these results. They have been demonstrated to be valid only up to $\beta = 0.4$ and for straight afterbodies with no fins or boattails. A variety of nose configurations are represented in the experimental data: cones, tangent-ogives, Haack-Sears, and others. At these low angles of attack the Magnus force would not be expected to depend

strongly on the particular shape chosen¹⁸, and indeed this appears to be the case for the shapes studied. The blunt or hemispherical nose was not examined.

It is the opinion of this author that the non-linear variation of $C_{y,p}$ with α in this small angle region is associated with the formation of the so-called body vortex. This begins near the base at angles of attack of about six degrees and as α increases it moves forward until it finally reaches the shoulder of the nose³⁷. If this were true, one would expect boattailing to have a strong influence on the behavior of $C_{y,p}$. This is indeed the case and has been previously reported by Platou²⁷ who states that a slight rounding of the corner of the base caused drastic changes in the Magnus force, even in some cases changing the sign.

Conclusions

1. Equation (32) with $k = 10$ will yield $C_{y,p}$ accurately enough for preliminary design calculations for pointed, slender bodies of revolution at small angles of attack, with $\bar{p} \leq 0.4$ and outside the transonic region.
2. Much work remains to be done before a method for calculating $C_{y,p}$ based on first principles is devised.
3. In the small angle-of-attack region the Magnus force does not depend strongly on the particular pointed nose that is chosen.
4. More work should be done in order to extend the applicability of equation (32) into the region where $C_{y,p}$ is a non-linear function of \bar{p} and if possible into the transonic region.

REFERENCES

1. Swanson, W. M., "The Magnus Effect: A Summary of Investigations to Date," J. of Basic Engineering, September 1961, p. 461.
2. Robbins, B., "New Principles of Gunnery," London, 1742.
3. Magnus, F., "On the Deflection of a Projectile," (a) "Abhandlung der Akademie der Wissenschaftern," Berlin, Germany, 1852, English translation in Taylor's Scientific Memoirs, 1853. (b) "Poggendorffs Annalen der Physik und Chemie, Vol. 88, No. 1, 1853.
4. Lord Rayleigh, "On the Irregular Flight of a Tennis Ball," (a) "Scientific Papers," Vol. 1, 1857, pp. 344-6. (b) "Messenger of Mathematics," Vol. 7, 1877, p. 14.
5. Lafay, "Sur l'Inversion du Phenomene de Magnus," Comptes Rendus, Vol. 151, 1910.
6. Lafay, "Contribution Experimentale a l'Aerodynamique du Cylindre," Revues Mechanique, Vol. 30, 1912.
7. Prandtl, L., "Magnuseffekt und Windkraftschiff," Die Naturwissenschaften, 1925, p. 93. English translation, NACA TM 367, 1926.
8. Buford, W. E., "Magnus Effect in the Case of Rotating Cylinders and Shell," Ballistic Research Laboratories, Aberdeen Proving Ground, Maryland, BRL Memorandum Report 821, 1954.
9. Wood, W. W., Boundary Layers Whose Streamlines are Closed. Aeronautical Research Laboratories, Fishermans Bend, Melbourne, Australia. September, 1956.
10. Glauert, M. B., The Flow Past a Rapidly Rotating Circular Cylinder. Royal Society of London Proceedings, Series A, 242:108-115. November, 1957.
11. Reid, E. G., "Tests of Rotating Cylinders," NACA TN 209, 1924.
12. Thom, A., "The Aerodynamics of a Rotating Cylinder," thesis, University of Glasgow, 1926.
13. Thom, A., "Experiments on the Air Forces on Rotating Cylinders," ARC R and M 1016, 1925.

14. Thom, A., "The Pressures Round a Cylinder Rotating in an Air Current," ARC R and M 1082, 1926.
15. Thom, A., "Experiments on the Flow Past a Rotating Cylinder," ARC R and M 1410, 1931.
16. Thom, A. and Sengupta, S. R., "Air Torque on a Cylinder Rotating in an Air Stream," ARC R and M 1520, 1932.
17. Thom, A., "Effects of Discs on the Air Forces on a Rotating Cylinder," ARC R and M 1623, 1934.
18. Green, John E., "A Summary of Experimental Magnus Characteristics of a 7- and 5-Caliber Body of Revolution at Subsonic through Supersonic Speeds," NAVORD Report 6110, U. S. Naval Ordnance Laboratory, White Oak, Maryland, 1958.
19. Fletcher, A. A. J., "Investigation of the Magnus Characteristics of a Spinning Inclined Ogive-Cylinder Body at $M = 0.2$," Australian Department of Supply, WRE Report HSA 159, 1969.
20. Luchuk, W. and Sparks, W., "Wind-Tunnel Magnus Characteristics of the 7-Caliber Army-Navy Spinner Rocket," NAVORD Report 3813, U. S. Naval Ordnance Laboratory, White Oak, Maryland, 1954.
21. Uselton, James C., and Carman, Jack B., "A Study of the Magnus Effects on a Sounding Rocket at Supersonic Speeds," J. Spacecraft and Rockets, Vol. 8, 1971, p. 28-34.
22. Hauer, H. J., and Kelly, Howard R., "The Subsonic Aerodynamic Characteristics of Spinning Cone-Cylinders and Ogive-Cylinders at Large Angles of Attack," NAVORD Report 3529, U. S. Naval Ordnance Test Station, China Lake, California, 1955.
23. Holmes, J. E., Regan, F. J., and Falusi, Mary Ellen, "Supersonic Wind Tunnel Magnus Measurements of the 7-, 8-, 9-, and 10-Caliber Army-Navy Spinner Projectile," NOLTR 68-172, U. S. Naval Ordnance Laboratory, White Oak, Maryland, 1968.
24. Martin, J. C., "On Magnus Effects Caused by the Boundary Layer Displacement Thickness on Bodies of Revolution at Small Angles of Attack," BRL Rep. 870, Dept. of the Army Proc. 5B03-03-001, Ord. Res. and Dev. Proj. TB3-0108, Aberdeen Proving Ground, Maryland, June, 1955.

25. Kelly, Howard R., "An Analytical Method for Predicting the Magnus Forces and Moments on Spinning Projectiles," TM-1634, U. S. Naval Ordnance Test Station, China Lake, California, 1954.
26. Kelly, Howard R., and Thacker, G. Robert, "The Effect of High Spin on the Magnus Force on a Cylinder at Small Angles of Attack," NAVORD Report 5036, U. S. Naval Ordnance Test Station, China Lake, California, 1956.
27. Platou, Anders S., "Magnus Characteristics of Finned and Non-Finned Projectiles," AIAA Journal, Vol. 3, January, 1965, p. 83.
28. Iverson, James D., "Correlation of Magnus Force Data for Slender Spinning Cylinders," AIAA Paper No. 72-966, September 1972.
29. Power, H. L., and Iverson, J. D., "The Magnus Effect on Spinning Bodies of Revolution," NTIS Paper N 73-11998, November 1972.
30. Gowen, F. E. and Perkins, E. W., Flow Over Inclined Bodies, NACA RM A51J25, Ames Aeronautical Laboratory, Moffett Field, California. March, 1954.
31. Dunn, E. L., A Low-Speed Experimental Study of Yaw Forces on Bodies of Revolution at Large Angles of Pitch and Zero Angle of Slide-slip, TM-1588, U. S. Naval Ordnance Test Station, China Lake, California. March, 1954.
32. Kelly, H. R., The Estimation of Normal-Force, Drag, and Pitching Moment Coefficients for Blunt-Based Bodies of Revolution at Large Angles of Attack. Journal of the Aeronautical Sciences 21:549. August, 1954.
33. Thoman, D. C., and Szewczyk, A. A., "Numerical Solutions of Time Dependent Two-Dimensional Flow of a Viscous Incompressible-Fluid Over Stationary and Rotating Cylinders," Technical Report 66-14, Department of Mechanical Engineering, University of Notre Dame, 1966.
34. Seban, R. A., and Bond, R., "Skin-Friction and Heat Transfer Characteristics of a Laminar Boundary Layer on a Cylinder in Axial Incompressible Flow." J. Aeronaut. Sci., Vol. 16, No. 10, p. 671, October 1951.

35. Dunn, E. L., and Kelly, H. R., "The Displacement Effect of a Three-Dimensional Boundary Layer of Moderate Thickness." Naval Ordnance Test Station, China Lake, California, 25 June 1954, NOTS TM-1615.
36. Nash, J. F., and Patel, V. C., Three-Dimensional Turbulent Boundary Layers, SBC Technical Books, Scientific and Business Consultants, Inc., Atlanta, Ga. 1972.
37. Neilsen, J. N., Missile Aerodynamics, McGraw-Hill Book Co., Inc. New York, N. Y. 1960.
38. Krahn, E., "Negative Magnus Force." Journal of Aeronautical Sciences, Vol. 23, p. 377, April 1956.

INITIAL DISTRIBUTION

Hq USAF/SAMI	1
ASD/ENYS	1
AUL (AUL/LSE-70-239)	1
DDC	2
NASA Ames	1
USNWL	1
AEDC/ARO, Inc	1
Director, Rsch Lab/Aerodynamics	
Rsch Gp, Edgewood Ars	1
Army Missile Comd/AMSNI-RDK	1
AFFDL/Tech Library	1
USAF/Tech Library	1
USNOL/Aerodynamics Dept	1
Director, Army Material Analysis	
Agcy, Aberdeen Pg Gd	1
Univ of Florida/Engineering	
Sciences Dept	5
Hq 4950 TESTW/TZIM	1
TANC/TRADOCLO	1
AFATL/DIOSL	2
AFATL/DL	1
AFATL/DLY	1
AFATL/DLD	1
AFATL/DLDL	1
AFATL/DLNA	10

UNCLASSIFIED

Security Classification

DOCUMENT CONTROL DATA - R & D

(Security classification of title, body of abstract, and indexing classification must be entered when the overall report is classified)

1. ORIGINATING ACTIVITY (Corporate author) Eglin Graduate Center, College of Engineering, University of Florida Eglin Air Force Base, Florida 32542		2a. REPORT SECURITY CLASSIFICATION Unclassified	
		2b. GROUP	
3. REPORT TITLE METHODS FOR CALCULATING MAGNUS FORCES ON SLENDER BODIES OF REVOLUTION			
4. DESCRIPTIVE NOTES (Type of report and inclusive dates) Final Report - February 1972 to February 1974			
5. AUTHOR(S) (First name, middle initial, last name) J. E. Milton			
6. REPORT DATE February 1974		7a. TOTAL NO OF PAGES 52	7b. NO OF REFS
8a. CONTRACT OR GRANT NO F08635-70-C-0065		8b. ORIGINATOR'S REPORT NUMBER(S)	
9. PROJECT NO 2069			
10. Task No. 01		9b. OTHER REPORT NUMBER (Any other numbers that may be assigned this report)	
11. Work Unit No. 003		AFATL-TR-74-51	
12. DISTRIBUTION STATEMENT Distribution limited to U. S. Government agencies only; this report documents test and evaluation; distribution limitation applied February 1974. Other requests for this document must be referred to the Air Force Armament Laboratory (DLNA), Eglin Air Force Base, Florida 32542.			
13. SUPPLEMENTARY NOTES Available in DDC		14. SPONSORING/MONITORING ACTIVITY Air Force Armament Laboratory Air Force Systems Command Eglin Air Force Base, Florida 32542	
15. ABSTRACT Theories for predicting the Magnus force for slender, pointed bodies of revolution at small angle of attack and small spin rates are reviewed. A semi-empirical method for calculating $C_{y,p}$ is discussed and shown to be applicable to a variety of bodies and experimental situations.			

UNCLASSIFIED

Security Classification

14	KEY WORDS	LINK A		LINK B		LINK C	
		ROLE	WT	ROLE	WT	ROLE	WT
	Calculating Magnus Forces Slender Bodies of Revolution Pointed Bodies of Revolution Magnus Force Magnus Effect						

UNCLASSIFIED

Security Classification